

ADA047157

VOLUME I

Final Report On

Multiple Beam Torus Antenna Study

Prepared for

Defense Communications Agency

Under

Contract DCA100-76-C-0050

March 1977

by

COMSAT Laboratories

Clarksburg, Maryland 20734

D D C
P R O C E D U R E
D E C 1 1977
D I S C L O S U R E
F

Carol Rieger
Carol Rieger
Principal Mechanical/
Structures Engineer

William J. English
William J. English
Principal RF Engineer

Paul Schrantz
Paul Schrantz
Manager, Stabilization
and Structures

Ronald Kreuter
Ronald Kreuter
Manager, Antenna
Department

READ INSTRUCTIONS
BEFORE COMPLETING FORM

1. REPORT NUMBER

2. GOVT ACCESSION NO. 3. RECIPIENT'S CATALOGUE NUMBER

4. TITLE (incl. edition)

Final Report on Multiple Beam Torus Antenna
Study. Volume I.

5. TYPE OF REPORT & PERIOD COVERED

Final Report, covering
Jul 76 to Feb 7710. NAME OF J. / English
Carol Rieger

5. PERFORMING ORGANIZATION NAME AND ADDRESS

COMSAT Laboratories
Clarksburg, MD 20734

6. CONTRACT OR GRANT NUMBER(S)

DCA108-76-C-5558 *new*

11. CONTROLLING OFFICE NAME AND ADDRESS

Defense Communications Engineering Center, DC
1860 N. Glebe Avenue
Arlington, VA 22209

12. REPORT DATE

March 1977

13. NUMBER OF PAGES

Vol 1 - 42 pgs.

14. MONITORING AGENCY NAME & ADDRESS (if different from Controlling Office)

12 S.P.

15. SECURITY CLASSIFICATION OF REPORT

Unclassified

16. DECLASSIFICATION/DEMATERIALIZING SCHEDULE

17. DISTRIBUTION STATEMENT (for this Report)

Approved for Public Release -- Distribution Unlimited

18. SITE 19. AD-E100 000

20. DISTRIBUTION STATEMENT (if the address entered in Block 19, is different from Report)

21. SUPPLEMENTARY NOTES

22. KEY WORDS (Continue on reverse side if necessary and identify by block number)

Multiple Beam Torus Antennas (MBTA), Satellite Communications, Satellite earth terminal, Multibeam/Multi frequency

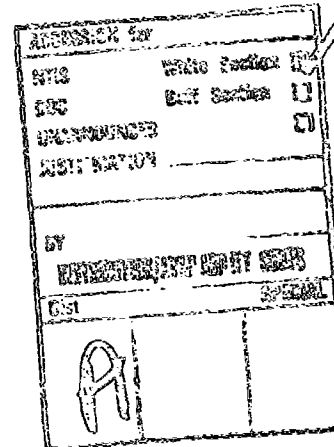
23. ABSTRACT (Continue on reverse side if necessary and identify by block number)

Offset-fed multiple beam torus antennas (MBTA) provide exceptional wide-angle sidelobe characteristics as a result of a blockage-free aperture. The form of multiple beams at one or more frequency bands using shared apertures on a fixed reflector structure can result in significant cost savings in a DSCS system in which satellites are constrained to a fixed portion of the geosynchronous arc.

405 867

FOREWORD

This report was prepared by COMSAT Laboratories, Clarksburg, Maryland 20734, under Defense Communication Agency Contract DCA100-76-C-0050. Dr. Robert Sims and Mr. Larry Krebs of the Defense Communications Engineering Center, Reston, Virginia, were the technical monitors of the program for the Defense Communications Agency. The principal engineers for the study program were Dr. William J. English(RF) and Mrs. Carol Rieger (Mechanical/Structures) of the Microwave and Spacecraft Laboratories, respectively, of COMSAT Laboratories. Mr. David Perlmutter provided a portion of the cost analysis. The MBTA concept for geosynchronous satellite coverage was initially developed under a COMSAT corporate research and development program. This report covers the period from July 1976 through February 1977.



ABSTRACT

Offset-fed multiple beam torus antennas (MBTAs) provide exceptional wide-angle sidelobe characteristics as a result of a blockage-free aperture. The formation of multiple beams at one or more frequency bands using shared apertures on a fixed reflector structure can result in significant cost savings in a DSCS system in which satellites are constrained to a fixed portion of the geosynchronous arc.

The MBTA geometry provides a conical beam scan locus which closely approximates the curvature of the geostationary arc. A parabolic generating curve and feed position are revolved about a rotation axis to form the reflector surface. For geosynchronous applications, the optimal reflector generating axis angle, θ_0 , between the rotation axis and beam direction varies from 90° for MBTAs located at the equator to 93.5° for those close to the polar regions.

The study results have shown that a single reflector design defined by $\theta_0 = 93.5^\circ$ is applicable to a widely deployed DSCS earth station antenna system. This reflector design results in less than 0.3° of worst-case beam pointing error with spherical plane scan over a 40° field of view. This beam scan error represents less than 1-2 beamwidths of required parabolic plane scan for exact beam repositioning in MBTAs having 54- to 59-dB gain; therefore, a single reflector design can be utilized to minimize fabrication costs with negligible impact on RF performance.

The identical reflector surface is utilized at all DSCS MBTA locations. The reflector support structure lengths vary to accommodate different MBTA latitude and longitude locations.

The minimum spacing between adjacent beams along the geostationary arc, which is constrained by the physical diameter of the feed horn aperture, is approximately 2-4 antenna half-power beamwidths depending upon the type of feed horn used. The minimum beam spacing is 1.2° with 54-dB receive gain.

The MBSA provides low sidelobes and a multibeam/multi-frequency capability in a simple, rugged, and reliable fixed mechanical structure. Its modular design facilitates transportation and erection. Additional beams require only a relatively inexpensive feed system and feed transport assembly. Redundant electronic equipment can be readily shared between multiple beams, further increasing overall system economy. The MBSA feed building incorporates all of the earth station elements except the reflector in a locked secure structure.

The primary advantages of the baseline MBSA identified in this study for geosynchronous DSCS satellite applications are as follows:

- a. exceptional RF performance in critical areas, particularly sidelobes and multi-frequency operation from 3.7-31 GHz;
- b. simplicity and reliability inherent in a fixed reflector with modular construction; and
- c. cost savings in multiple-beam and/or multiple-frequency-band applications.

Table of Contents

	<u>Page No.</u>
VOLUME I	
1. INTRODUCTION	1-1
1.1 Task 1: MSTA Characteristics at Government Satellite Communications Frequencies	1-1
1.2 Task 2: MSTA Characteristics for Combined Operation at Both Government and Commercial Satellite Frequencies	1-2
1.3 Task 3: MSTA Mechanical and Structural Characteristics Required for a Worldwide Deployment System	1-3
1.4 Task 4: Cost Estimate for a Recoverable MSTA	1-3
2. THE MULTIPLE BEAM TORUS ANTENNA CONCEPT	2-1
3. SUMMARY OF MAJOR STUDY RESULTS AND GENERAL RECOMMENDATIONS	3-1
3.1 RF Performance	3-1
3.2 Structural, Mechanical, and Cost Considerations	3-19
3.3 Task 1: MSTA Characteristics at Government Satellite Communications Frequencies	3-30
3.4 Task 2: MSTA Characteristics for Combined Operation at Both Government and Commercial Satellite Frequencies	3-33
3.5 Task 3: MSTA Mechanical and Structural Characteristics Required for a Worldwide Deployment System	3-36

Table of Contents (Continued)

	<u>Page No.</u>
3.6 Task 4: Cost Estimates for a Recoverable Torus 3.7 Conclusions VOLUME II	3-37 3-38
4. GEOMETRICAL AND BEAM POINTING CONSIDERATIONS 4.1 Local Elevation and Azimuth Angles for Beam Pointing 4.2 Between Local Horizon and Beam "Plane" Vectors 4.3 Derivation of Optimum Rotation Axis Angle, θ_0 4.4 Pointing Effects of a Single Fixed θ_0 Geometry 5. ELECTRICAL (RF) PERFORMANCE CHARACTERISTICS 5.1 Basic Frequency Considerations 5.2 Basic Aperture Diameter, Gain, and Beam- width Considerations 5.3 Symmetrical RFM Field of View, Focusing, and Feed Illumination Angle Parameters 5.4 Offset Reflector Feed Pointing and Illumination Angles 5.5 Feed Characteristics and Minimum Beam Spacings 5.6 RF Surface Tolerance Losses 5.7 Mathematical Expression for Rotated Parabolic Section viii	4-1 4-1 4-6 4-14 4-24 5-1 5-1 5-2 5-3 5-13 5-22 5-29 5-29

Table of Contents (Continued)

	<u>Page No.</u>
3.8 Aperture Plane Spherical Aberration	
Phase Errors	3-34
3.9 Parabolic Plane Scanned Beam Feed Post-	
tions and Scan Gain Loss	3-35
3.10 Spherical Generating Curve MFTA	3-36
3.11 Illumination Gain of Front-Fed MFTA	3-63
3.12 Offset MFTA Field of View and Scanned	
Feed Parameters	3-66
3.13 Patterns and Polarization	3-76
3.14 Noise Temperature and Feed Spillover	3-81
3.15 Aberration-Correcting Subreflector	3-94
3.16 Aberration-Correcting Feeds	3-98
6. MECHANICAL AND STRUCTURAL CHARACTERISTICS OF	
THE INTEGRATED FRONT-FED MFTA	6-1
6.1 Worldwide Deployment Considerations	6-2
6.2 Mechanical Considerations	6-7
6.3 Structural Design Considerations	6-13
6.4 Applied Loads Analysis	6-18
6.4.1 Gravity	6-18
6.4.2 Wind	6-18
6.4.3 Temperature	6-20
6.5 Allowable Deformation and Tilt Error	
Budget	6-20
6.5.1 Surface rms	6-20
6.5.2 Rotating Error	6-21
6.6 Structural Model	6-22
6.6.1 Panels	6-23
6.6.2 Backup Structure	6-26
6.6.3 Support Points	6-29

Table of Contents (Continued)

	<u>Page No.</u>
6.7 Structural Layout	6-33
6.8 Load Analysis	6-36
6.9 Static Analysis	6-41
6.10 Dynamic Analysis	6-44
6.11 Stress Analysis	6-46
 7. COST ESTIMATES FOR A RECOVERABLE MDR	 7-1
 8. REFERENCES	 8-1
 APPENDIX A. DEVICE DESCRIPTIONS	 A-1

List of Illustrations

<u>Figure No.</u>	<u>Title</u>	<u>Page No.</u>
VALLEY 2		
2-1	32- x 33-ft NERA at COMSAT Laboratories	2-2
2-2	NERA GEOMETRY	2-3
2-3	Earth Station Antenna Beam Scan Requirements	2-4
2-4	Offset NERA GEOMETRY	2-6
2-5	Spherical Plane Cross Section of Symmetrical NERA	2-8
2-6	Rotation Axis Angle, θ_0	2-9
2-7	Equatorial and Polar Limits on the Rotation Axis Angle, θ_0	2-10
2-8	COMSAT Laboratories NERA	2-12
2-9	Typical 4-Panel Generating Trans	2-14
2-10	NERA Structural Support	2-15
2-11	Poured-Concrete NERA Foundation	2-16
2-12	Back View of Reflector Supports and Foundation	2-17
2-13	Beam Pointing and ZNE Surface Errors	2-19
2-14	Normalized Wind Moment Area $\{ (W^2) / (W^2) \}$	2-20
2-15	NERA Orientation at Different Earth Locations	2-21
3-1	Geosynchronous Satellites Launched or to be Launched After January 1, 1976	3-3
3-2	Illumination Gain and Beamwidth versus D/L of a Parabolic Reflector	3-4

List of Illustrations (Continued)

<u>Figure No.</u>	<u>Title</u>	<u>Page No.</u>
3-3	Illumination Gain of Offset NETA versus D/λ with Fixed Radius of Curvature (D/R) = 1	3-3
3-4	Diameter, D, versus D/λ for Minimum Down- Link and Maximum Up-Link Frequencies	3-7
3-5	NETA Surface Tolerance Gain Losses	3-8
3-6	NETA Field of View (FOV) versus the Ratio of Aperture Plane Dimensions, X/D	3-9
3-7	NETA Antenna Noise Temperature at X-Band ..	3-11
3-8	Baseline NETA (D/R = 0.4) Illumination Gain from 3.7-3L GHz	3-12
3-9	Baseline 27-ft-Diameter NETA Pattern at 7.3 GHz ($\phi = 90^\circ$)	3-13
3-10	Baseline 27-ft-Diameter NETA Pattern at 7.3 GHz ($\phi = 0^\circ$)	3-14
3-11	Aperture Illumination Gain and Beamwidth versus D/λ for D/R = 0.3 NETA Geometry	3-15
3-12	Single Reflector ($\theta_0 = 93.5^\circ$; NETA Point- ing Error with Spherical Scan	3-16
3-13	Widely Deployed Representative Antenna Locations	3-23
3-14	Views of NETA at Sweden and Mt. Hafjell ($\phi_{sat} = 333^\circ$ east longitude)	3-24
3-15	Views of NETA at Ascension Island and Iceland ($\phi_{sat} = 333^\circ$ east longitude)	3-25
3-16	Feed Tower Width x Maximum Height versus NETA Location	3-26
3-17	Projected Feed Arc Length, L/D	3-27
3-18	Feed Transport Assembly	3-28

List of Illustrations (Continued)

<u>Figure No.</u>	<u>Title</u>	<u>Page No.</u>
3-19	Views of 27-ft Diameter ($D/R = 0.4$) and 48-ft Diameter ($D/R = 0.3$) MBTA Geometries at COMSAT Laboratories	3-29
3-20	MBTA Costs versus Size and Operational Surface Tolerance	3-31

VOLUME II

4-1	MBTA Beam Elevation Angle vs Latitude and Differential Longitude	4-3
4-2	Sum of Beam Elevation and Latitude Angles $01.3^\circ \leq e + v \leq 90^\circ$ at Co-longitude Position	4-4
4-3	Local MBTA Beam Pointing Azimuth Angle	4-4
4-4	Right Spherical Triangle Relationships	4-5
4-5	Plane Geometry Angle Relationships	4-7
4-6	Horizon Vector \hat{q} and Scan "Plane" Vector \hat{p} in MBTA Aperture Plane	4-8
4-7	Geometry for Beam Pointing Vector, \hat{R}	4-9
4-8	MBTA Local North Vector	4-12
4-9	Local Orientation of \hat{p} and \hat{q} Unit Vectors	4-13
4-10	Conical Beam Scan Locus	4-15
4-11	Map of Optimum MBTA Generating Axis Angles, Φ_0	4-19
4-12	Optimum Φ_0 Angle vs Latitude at Co-longitude Position	4-20
4-13	Rotation Axis Inclination Angle	4-21

List of Illustrations (Continued)

<u>Figure No.</u>	<u>Title</u>	<u>Page No.</u>
4-14	Rotation Axis Inclination Angle vs Latitude at the Co-longitude Position	4-22
4-15	Beam Pointing Loci with Scan	4-23
4-16	Beam Pointing Locus with θ_0 Fixed	4-25
4-17	$\Phi(\theta_0)$ for $\theta_0 = 90^\circ$, $\lambda = 0^\circ$	4-29
4-18	$\Phi(\theta_0)$ for $\theta_0 = 93^\circ$, $\lambda = 0^\circ$	4-30
4-19	$\Phi(\theta_0)$ for $\theta_0 = 93.5^\circ$, $\lambda = 0^\circ$	4-31
4-20	$\Phi(\theta_0)$ for $\theta_0 = 94^\circ$, $\lambda = 0^\circ$	4-32
4-21	$\Phi(\theta_0)$ for $\theta_0 = 95.5^\circ$, $\lambda = 0^\circ$	4-33
4-22	$\Phi(\theta_0)$ for $\theta_0 = 93.5^\circ$, $\lambda = 40^\circ$	4-34
4-23	$\Phi(\theta_0)$ for $\theta_0 = 93.5^\circ$, $\lambda = -70^\circ$	4-35
4-24	Rotation Axis Inclination in Co-longitude Plane with Fixed θ_0	4-37
4-25	Rotation Axis Vector Components	4-38
5-1	Illumination Gain and Beamwidth vs D/ λ	5-4
5-2	MBTA Diameter vs D/ λ at X-Band	5-6
5-3	Diameter vs D/ λ at Specified Frequencies ..	5-7
5-4	Symmetrical MBTA Field of View Parameters	5-8
5-5	Symmetrical MBTA Field of View vs W/D at Specified Radius of Curvature (R/D)	5-10
5-6	Spherical Reflector Focusing	5-11
5-7	Symmetrical MBTA Feed Illumination Angle vs D/R	5-14
5-8	Projected Length of Feed Arc for 27-ft-Diameter Symmetrical MBTA	5-16
5-9	Offset MBTA Feed Illumination and Pointing Angles	5-18

List of Illustrations (Continued)

<u>Figure No.</u>	<u>Title</u>	<u>Page No.</u>
5-10	Feed Illumination Angle	5-19
5-11	Feed Offset Angle [$\theta_{\text{offset}} = \theta_1$ + $(\theta_2 - \theta_1)/2$]	5-20
5-12	Feed Offset Angle ($\theta_{\text{offset}} \rightarrow$ center of projected aperture)	5-21
5-13	Minimum MBTA Beam Spacing	5-24
5-14	Corrugated Feed Horn Patterns	5-25
5-15	Feed Power Patterns [$-P(\theta) = \cos^2n (x\theta)$] ..	5-26
5-16	6-GHz Corrugated Horn Antenna System	5-27
5-17	4-GHz Lightweight Corrugated Horn	5-28
5-18	Gain Loss vs Normalized rms Surface Toler- ance for Fixed Feed Offset Angles	5-29
5-19	Gain Loss of Baseline MBTA vs rms Surface Tolerance	5-31
5-20	Geometry for MBTA Reflector Equation	5-32
5-21	Symmetrical Spherical Reflector Geometry ..	5-35
5-22	Offset MBTA Reflector Geometry ($\phi_0 = 90^\circ$)	5-38
5-23	Symmetrical MBTA ($D/R = 0.4$) Aperture Plane Phase Errors	5-42
5-24	Symmetrical MBTA ($D/R = 0.4$) Gain vs F/R ..	5-43
5-25	Offset (118) MBTA ($D/R = 0.4$) Aperture Plane Phase Errors	5-44
5-26	Offset (118) MBTA Aperture Illumination Gain vs (F/R)	5-46
5-27	Offset (226) MBTA ($D/R = 0.4$) Aperture Plane Phase Errors	5-47
5-28	Offset (118) MBTA ($D/R = 0.3$) Aperture Plane Phase Errors	5-48

List of Illustrations (Continued)

<u>Figure No.</u>	<u>Title</u>	<u>Page No.</u>
5-29	Offset (11c) MBTA (D/R = 0.4) Aperture Plane Phase Errors with Optimum Focusing ..	5-49
5-30	Gain vs Feed Illumination Angle at 30 GHz (baseline MBTA)	5-50
5-31	Offset (11c) MBTA (D/R = 0.5) Aperture Plane Phase Errors with Optimum Focusing ..	5-51
5-32	Gain vs Feed Illumination Angle at 30 GHz (D/R = 0.5 geometry)	5-52
5-33	Geometry for General ϕ_0 Reflector Surface	5-54
5-34	Scanned Beam Feed Positions for Baseline MBTA	5-57
5-35	Parabolic Plane Beam Scan Loss for Base- line MBTA at 8.13 GHz	5-58
5-36	MBTA with Spherical Generating Curve	5-59
5-37	Aperture Plane Phase Error vs Feed Focus- ing with Spherical Generating Curve (D/R = 0.4)	5-61
5-38	Aperture Plane Phase Error vs Feed Focus- ing with Spherical Generating Curve (D/R = 0.3)	5-62
5-39	MBTA Illumination Gain vs D/λ	5-64
5-40	Aperture Illumination Gain vs Feed Edge Taper	5-65
5-41	Aperture Illumination Gain vs Feed Offset Angle	5-65
5-42	Aperture Illumination Gain (S = 27 ft) vs Frequency	5-66
5-43	Projected Aperture Area of MBTA	5-68

List of Illustrations (Continued)

<u>Figure No.</u>	<u>Title</u>	<u>Page No.</u>
5-44	Illumination Gain with Equal Projected Area Contours	5-69
5-45	Feed Pointing Parameters for Offset MBTA ..	5-71
5-46	10-Percent Offset MBTA Field of View vs (W/D)	5-72
5-47	Scanned Beam Feed Position Geometry	5-74
5-48	Baseline MBTA Pattern ($\phi = 90^\circ$)	5-77
5-49	Baseline MBTA Pattern ($\phi = 0^\circ$)	5-78
5-50	Baseline MBTA Receive Band Pattern at 7.5 GHz ($\phi = 90^\circ$)	5-79
5-51	Baseline MBTA Receive Band Pattern at 7.5 GHz ($\phi = 0^\circ$)	5-80
5-52	Baseline MBTA Receive Band Pattern at 3.95 GHz ($\phi = 90^\circ$)	5-82
5-53	Baseline MBTA Receive Band Pattern at 3.95 GHz ($\phi = 0^\circ$)	5-83
5-54	Baseline MBTA Receive Band Pattern at 11 GHz ($\phi = 90^\circ$)	5-84
5-55	Baseline MBTA Receive Band Pattern at 11 GHz ($\phi = 0^\circ$)	5-85
5-56	Baseline MBTA Receive Band Pattern at 20.7 GHz ($\phi = 90^\circ$)	5-86
5-57	Baseline MBTA Receive Band Pattern at 20.7 GHz ($\phi = 0^\circ$)	5-87
5-58	48-ft-Diameter MBTA (D/R = 0.3) Pattern at 8.15 GHz ($\phi = 90.2^\circ$)	5-88
5-59	48-ft-Diameter MBTA (D/R = 0.3) Pattern at 8.15 GHz ($\phi = 0^\circ$)	5-89
5-60	Offset MBTA D/R = 0.3 Geometry	5-90

List of Illustrations (Continued)

<u>Figure No.</u>	<u>Title</u>	<u>Page No.</u>
5-61	Spillover Characteristics of Corrugated Feed Horn for Baseline MSTA	5-92
5-62	Extended MSTA Aperture Area Decreases Feed Spillover	5-93
5-63	MSTA Antenna Temperature at X-Band	5-94
5-64	MSTA with Phase Corrective Subreflector	5-95
5-65	Correcting Subreflector Diameter in Geo-synchronous Plane Limits Minimum Beam Spacing	5-97
5-66	Phase-Corrective Subreflector Designed and Tested at COMSAT Laboratories	5-98
5-67	Primary Pattern Characteristics of Aberration-Correcting Feed System	5-100
5-68	3-Element Aberration-Correcting Feed Array	5-101
5-69	Primary Pattern Characteristics of 3-Element Aberration-Correcting Feed	5-103
5-70	7- (or 5-) Element Aberration-Correcting Feed Array	5-104
5-71	Symmetrical MSTA Patterns ($D/R = 0.4$, $D/\lambda = 1000$) with 5-Element Aberration-Correcting Feed	5-105
5-72	Offset MSTA Patterns ($D/R = 0.4$, $D/\lambda = 820$) with 4-Element Aberration-Correcting Feed	5-106
6-1	Offset Feed Configuration	6-3
6-2	Circular Angle of Generation	6-3
6-3	Typical 4-Panel Generating Truss	6-4
6-4	Coordinate System Rotation Angles	6-6

List of Illustrations (Continued)

<u>Figure No.</u>	<u>Title</u>	<u>Page No.</u>
6-5	Gain Loss of NBTA vs rms Surface Tolerance, ϵ	6-9
6-6	NBTA with Radome Environmental Protection	6-10
6-7	Existing Feed Transport Mechanism Support	6-11
6-8	Orthogonal View of Feed Transport Mechanism Support	6-12
6-9	Reflector Geometry	6-13
6-10	27-ft NBTA Reflector Panel Configuration ..	6-14
6-11	Detail of Backup Truss Members	6-16
6-12	4-Point Pickup Support Structure	6-17
6-13	6-Point Pickup Support Structure	6-17
6-14	Normalized Projected Area $(A/(W \times D))$	6-19
6-15	Equivalent Plate Thickness	6-23
6-16	Reflector Panel Cross Section	6-27
6-17	Panel Configurations	6-28
6-18	Vertical Truss Configurations	6-30
6-19	Typical Panel Layout	6-31
6-20	NASTRAN Plot of Backup Structure	6-32
6-21	View of COMSAT UER Torus Antenna During Construction	6-34
6-22	Normalized Wind Moment Area $\{(A \times H)/(W \times D^2)\}$	6-35
6-23	NASTRAN Plate Element Numbering	6-37
6-24	NASTRAN Backup Truss Grid Point Number- ing Scheme	6-38
6-25	NASTRAN Foundation Grid Point Layout	6-39

List of Illustrations (Continued)

<u>Figure No.</u>	<u>Title</u>	<u>Page No.</u>
6-26	Flow Chart of Design Iterations	6-43
6-27	Surface Tilt and mas Deformation	6-47
7-1	Fabrication Costs vs Surface Area	7-2
7-2	Erection Costs vs Surface Area	7-3
7-3	Width vs Location	7-5
7-4	Height vs Location	7-6
7-5	De-icing Costs per Square Foot vs Surface Area	7-7
7-6	Sizes of Several MBTA Reflectors at CORSAT Labs	7-16
7-7	Antenna Cost vs Surface Area	7-11
7-8	Views of 27-ft MBTA at Locations 1 and 2 ..	7-13
7-9	Views of 27-ft MBTA at Locations 3 and 4 ..	7-14

List of Tables

<u>Table No.</u>	<u>Title</u>	<u>Page No.</u>
VOLUME I		
3-1	Outline of MBTA Mechanical Specifications	3-20
3-2	27-ft MBTA Dimensions and Cost at Several Locations	3-32
3-3	Task 1a: Summary of Baseline MBTA RF Performance	3-33
VOLUME II		
4-1	Summary of Spherical Scan Beam Pointing Errors vs Field of View and Latitude ($\theta_0 = 93.5^\circ$)	4-34
5-1	Multiple Frequency Band Summary	5-3
6-1	Representative Sites for Worldwide MBTA Deployment	6-7
6-2	NASTRAN Load Cases	6-60
7-1	MBTA Dimensions and Cost (FOV = 30° , center frequency = 7.25 GHz)	7-9
7-2	27-ft MBTA Dimensions and Cost at Several Locations	7-12

1. INTRODUCTION

This final report presents the results of a 7-month study by COMSAT Laboratories of the applicability of the multiple-beam torus antenna (MBTA) to the present and future communications requirements of the Defense Satellite Communications System (DSCS). The study program had three major objectives:

- a. determination of the electrical (RF) performance parameters of MBTAs for application in the DSCS system,
- b. specification of MBTA mechanical and structural parameters required for a DSCS system to be deployed worldwide, and
- c. development of cost estimates for specific MBTA implementations which meet projected DSCS electrical and structural performance requirements.

The basic antenna design concept and a summary of the major study results and recommendations are presented in Volume I of this report. The detailed electrical, mechanical, and costing analysis of the MBTA is presented in Volume II. The study was performed as four separate tasks.

1.1 TASK I: MBTA CHARACTERISTICS AT GOVERNMENT SATELLITE COMMUNICATIONS FREQUENCIES

The first task was to define the characteristics of MBTAs at the government satellite communications frequencies so that the applicability of the torus concept to the needs of the DSCS could be determined. Electrical parameters for this study

task included but were not limited to antenna gain, beamwidth, and sidelobe levels, as well as estimated antenna noise temperature, insertion losses, passive intermodulation product levels, antenna polarization performance, and orbital arc coverage as a function of beamwidth and antenna dimensions. Mechanical parameters for this study task included wind and thermal loading constraints with resultant beam steering degradation and surface tolerances. Three specific cases were considered:

a. Torus antenna operation at X-band only (7.9 to 8.4 GHz up-link and 7.25 to 7.75 GHz down-link) without a corrective subreflector/feed system for spherical aberration.

b. Torus antenna operation at X-band only with a corrective subreflector/feed system for spherical aberration. This portion of the study addressed the cost/complexity/performance impact of aberration correction.

c. Torus antenna operation with different satellites at X-band and K-band (30 to 31 GHz up-link and 20.2 to 21.2 GHz down-link) without corrective subreflector/feed systems. Cost/complexity/reduced-aperture-efficiency tradeoffs at the K-band up-link frequencies were included.

In each case it was assumed that $\leq 0.25^\circ$ spacecraft north-south stationkeeping would be maintained. The impact of $\pm 0.5^\circ$, $\pm 1.0^\circ$, and $\pm 2.5^\circ$ orbital arc stationkeeping was also considered.

1.2 **TASK 2: HIGH CHARACTERISTICS FOR COMBINED OPERATION
AT BOTH GOVERNMENT AND COMMERCIAL SATELLITE FREQUENCIES**

The second task was to determine the cost and technical impact of combining commercial operation (via a separate commercial satellite) with simultaneous operation at the government

satellite communications frequencies. Electrical performance parameters delineated in task 1 were also determined for such combined operation.

1.3 TASK 3: MBEA MECHANICAL AND STRUCTURAL CHARACTERISTICS
REQUIRED FOR A WORLDWIDE DEPLOYMENT SYSTEM

The third task provided an evaluation of the effects of worldwide deployment on the fixed reflector structural geometry. The required structural configurations, including support towers, foundation considerations, erectability, and variable wind and thermal load factors, were considered for all DSCS sites where the elevation angle to a geostationary satellite is 5° or greater. In addition, the cost and technical impact of site/reflector tower commonality for installation at varying latitudes and differential longitudes were evaluated. Geographical extremes having a significant impact were identified, and significant variations in electrical parameters which result from worldwide deployment were noted.

1.4 TASK 4: COST ESTIMATES FOR A RECOVERABLE MBEA

The fourth task was to develop a rough cost estimate for a recoverable MBEA. Four specific torus antenna implementations were considered for costing analysis:

- a. dual-beam X-band configuration with 54-dB down-link gain at 7.25 GHz;
- b. dual-beam X-band configuration with 59-dB down-link gain at 7.25 GHz;
- c. dual-beam configuration with one beam at X-band and one beam at C-band and gains of 54 dB at 7.25 GHz and 49 dB at 3.7 GHz, respectively; and

c. dual-beam configuration with one beam at X-band and one at K-band, an X-band gain of 34 dB at 7.25 GHz, and K-band gains of 62 dB at 28.2 GHz (receive) and 64 dB at 30 GHz (transmit).

The implementation configurations chosen for costing were based on the results of tasks 1-3.

This final report incorporates the study results presented in the five monthly progress reports submitted to DCA, as well as a substantial amount of additional detailed analysis, problem descriptions, and assumptions. The close coordination established between DCA and CONSAT Laboratories throughout the study period was important in achieving a comprehensive study program directed specifically at evolving DCA antenna system requirements.

2. THE MULTIPLE-BEAM TORUS ANTENNA CONCEPT

The multiple-beam torus antenna¹⁻³ (MBTA) is a fixed reflector, multiple-beam antenna system developed at COMSAT Laboratories specifically for geosynchronous communications satellite applications.⁴⁻⁶ Fixed reflector antenna systems offer both attractive life cycle cost savings and exceptional performance characteristics when utilized with communications satellites assigned to orbital positions over a fixed portion of the geosynchronous arc. Figure 2-1 is a photograph of a 32- x 55-ft (9.6- x 16.5-m) MBTA designed and implemented at COMSAT Laboratories in 1973 to verify the operational performance characteristics of an offset-fed MBTA concept. This reflector system provides a 20° field of view (FOV) over the orbital arc from 18° to 38° west longitude. The feeds and their associated electronics are housed in an environmentally controlled feed tower shown in the photograph.

The MBTA reflector surface is generated by taking a section of a parabolic curve and rotating it about a fixed generating axis,^{7,8} as shown in Figure 2-2. The reflector consists of a parabolic section in one plane and spherical sections in the orthogonal planes. The spherical surface allows full beam scanning (or equivalently, the formation of multiple beams) over a portion of the geosynchronous arc. In the orthogonal plane, where only a limited amount of scan (a few beamwidths) is required to correct for diurnal variations and north-south station-keeping of a satellite, a parabolic surface is utilized to optimize the overall antenna system efficiency. Figure 2-3 shows the general beam scan requirements for the earth station antenna when satellite positions are constrained to a fixed portion of the geosynchronous arc.

Multiple Beam Torus
Antenna Study

COMSAT Labs

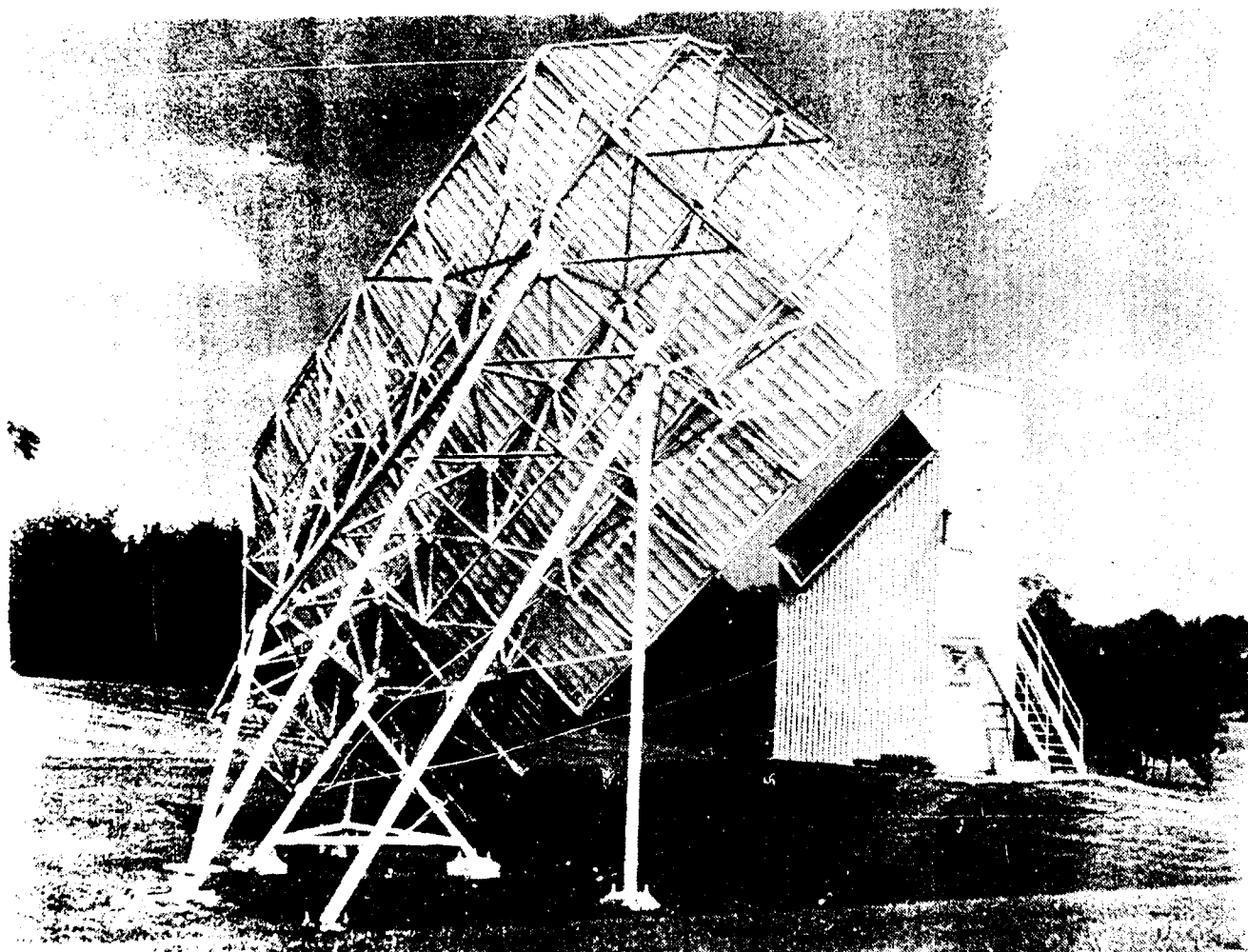


Figure 2-1. 32- x 55-ft MBTA at COMSAT Laboratories

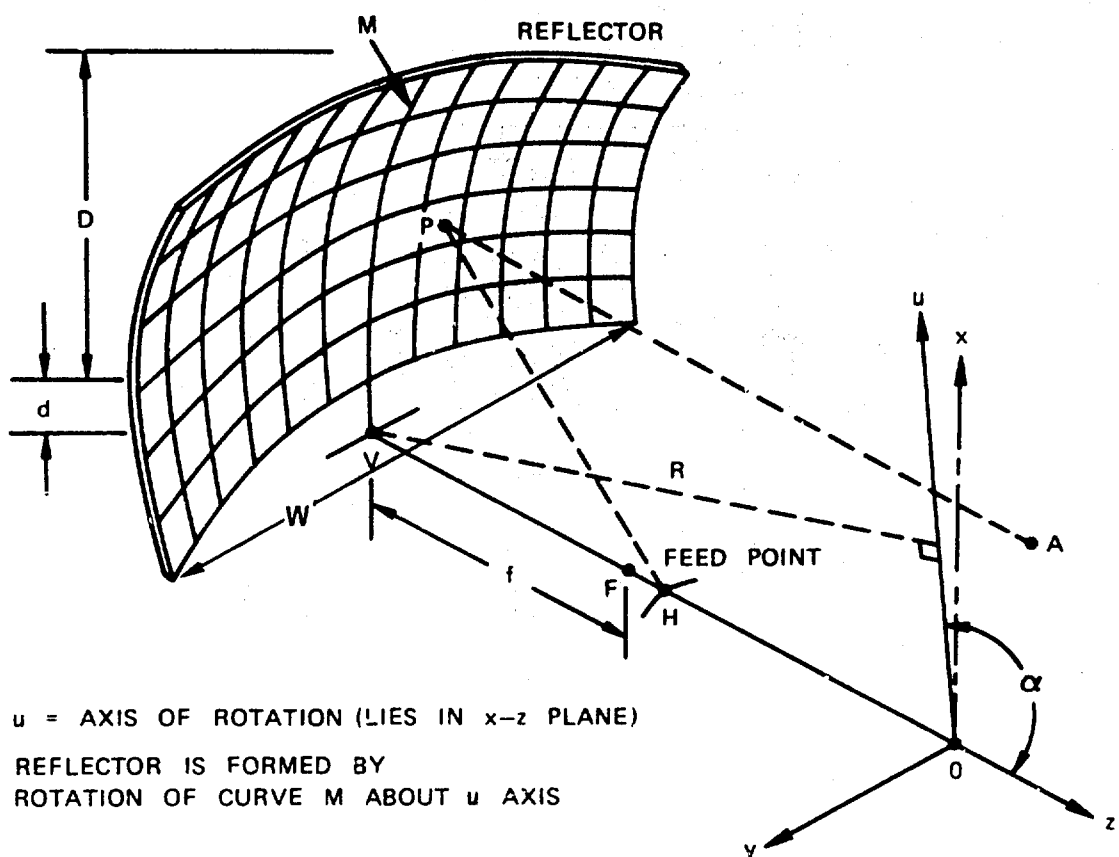


Figure 2-2. MBTA Geometry

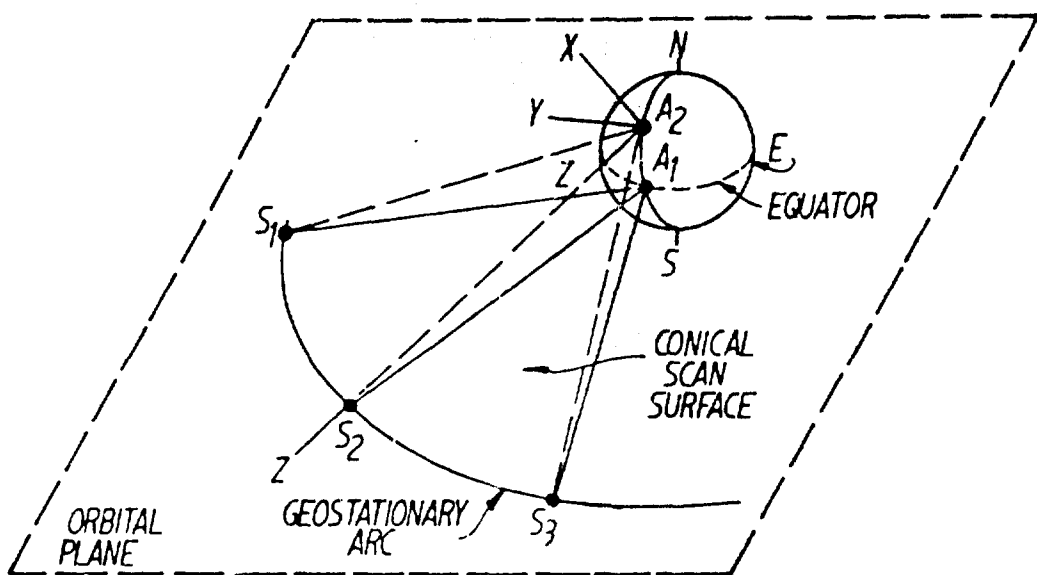


Figure 2-3. Earth Station Antenna Beam
Scan Requirements

The parabolic plane cross section of the MBTA geometry for an offset-fed implementation is shown in Figure 2-4 to illustrate the major antenna design parameters. An offset geometry with an unblocked aperture is preferred since it provides low wide-angle sidelobes, particularly in the geosynchronous orbit plane, thus minimizing interference problems with adjacent satellites. Excellent antenna noise temperature characteristics are also realized by using the offset-fed MBTA. The antenna system design parameters noted in Figure 2-4 are as follows:

- θ_0 Generating axis angle between the beam pointing direction and the axis of rotation. This angle is related to the amount of parabolic plane scan required for a scanned beam to follow the geosynchronous arc versus antenna location and field of view.
- D Basic aperture diameter (D/λ) determines gain and beamwidth).
- d Parameter determining the parabolic section offset required for a blockage-free aperture.
- D_0 Diameter of the "parent" parabola.
- $R(u)$ Rotation radius for spherical sections.
- D/R Parameter determining the "flatness" of the spherical portion of the reflector and relating the required field of view to the ratio of rectangular aperture dimensions (W/D).
- F parabolic section focal length.
- F/R Parameter chosen to place the parabolic focus at the best fit "spherical focus," i.e., to minimize composite aperture plane phase deviation from uniform.
- θ_{off} Offset feed pointing angle.
- $2\theta_F$ Included angle to the edge of the reflector for specified feed amplitude taper.
- x_F, y_F, z_F Feed positions relative to the parabolic section focus.

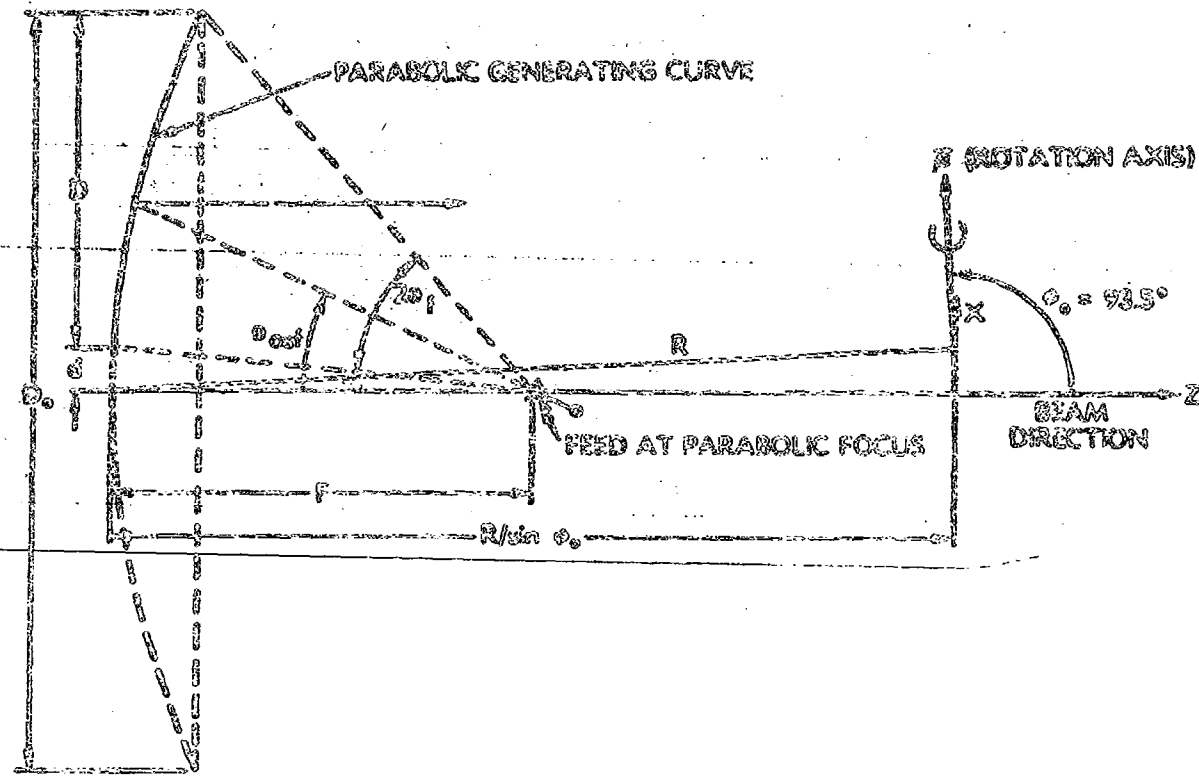
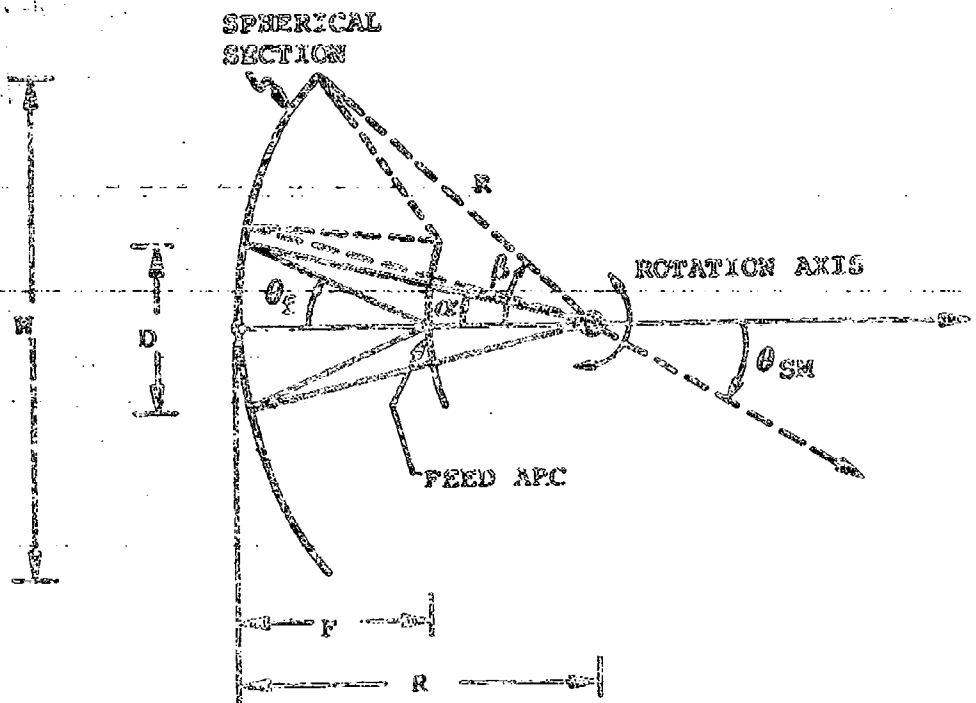


Figure 2-4. Offset NUTR Geometry

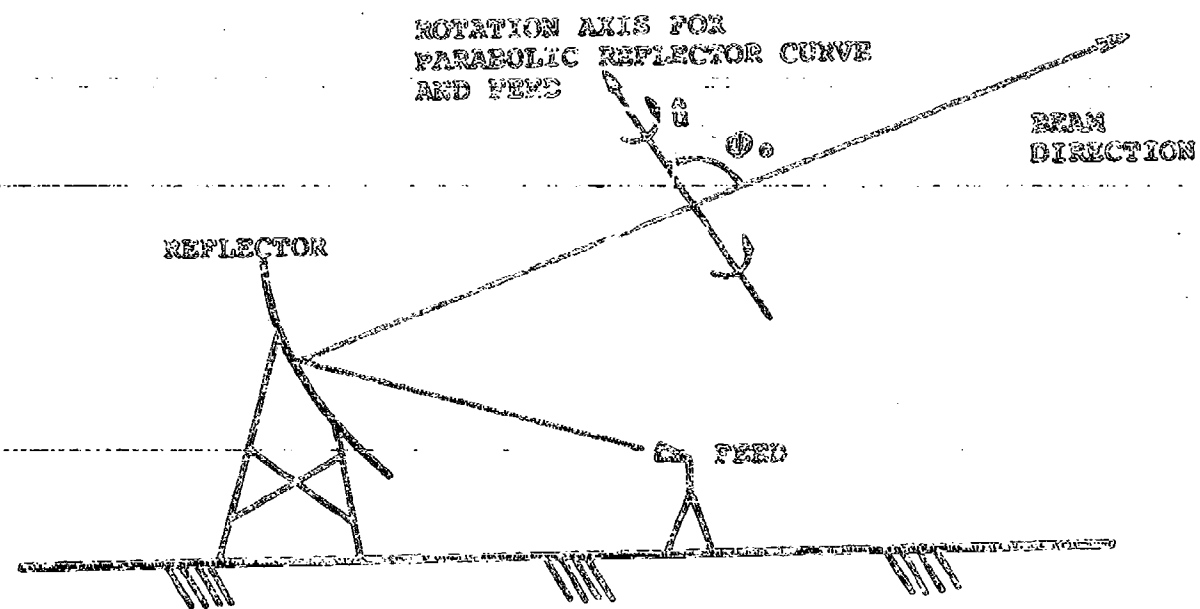
Figure 2-5 is a center cross section of a symmetrical MBTA indicating the scan plane characteristics associated with the spherical portion of the antenna. Feeds are scanned or positioned along a radial feed arc located approximately at the paraxial focus ($P/R = 0.5$) of the spherical reflector. The overall width, W , of the reflector surface is related to the desired field of view ($FOV = 2\theta_M$) and the radius of curvature, R (normalized to R/L). Beam characteristics are identical for all feed locations on the spherical feed arc. For a fixed field of view requirement, W decreases as the radius of curvature decreases. However, spherical aberration phase errors in the aperture plane also increase with a decreasing radius of curvature. Thus, there is a fundamental tradeoff between mechanical dimensions and electrical performance parameters. The magnitude of the spherical aberration phase errors is directly proportional to the diameter/wavelength (D/λ) ratio of the aperture. Hence, the choice of optimum mechanical design parameters is frequency dependent.

The torus antenna provides a conical beam scan surface which is designed to approximate the scan locus of a beam following the geostationary arc. The angle between the vertex of the cone (the rotation axis) and the conical scan surface (the locus of beam pointing directions) is given by ψ_0 , as shown in Figures 2-6 and 2-7. Optimum ψ_0 angles vary from 90° for an antenna location at the equator to an angle theoretically approaching 98.6° at the poles. (Antenna locations in this study are restricted by a minimum local elevation angle $\geq 5^\circ$.) The scanned beam pointing locus exactly follows the geostationary arc for the equatorial and polar antenna locations. The polar axis is the rotation axis for those locations. For an arbitrary antenna location, the conical beam scan locus provides a close approximation of the



$$\alpha = \sin^{-1} \left(\frac{D/2}{R} \right) \quad \theta_{SX} = \beta - \alpha$$
$$\beta = \sin^{-1} \left(\frac{W/2}{R} \right)$$

Figure 2-5. Spherical Plane Cross Section
of Symmetrical MBTA

Figure 2-6. Rotation Axis Angle, θ_0

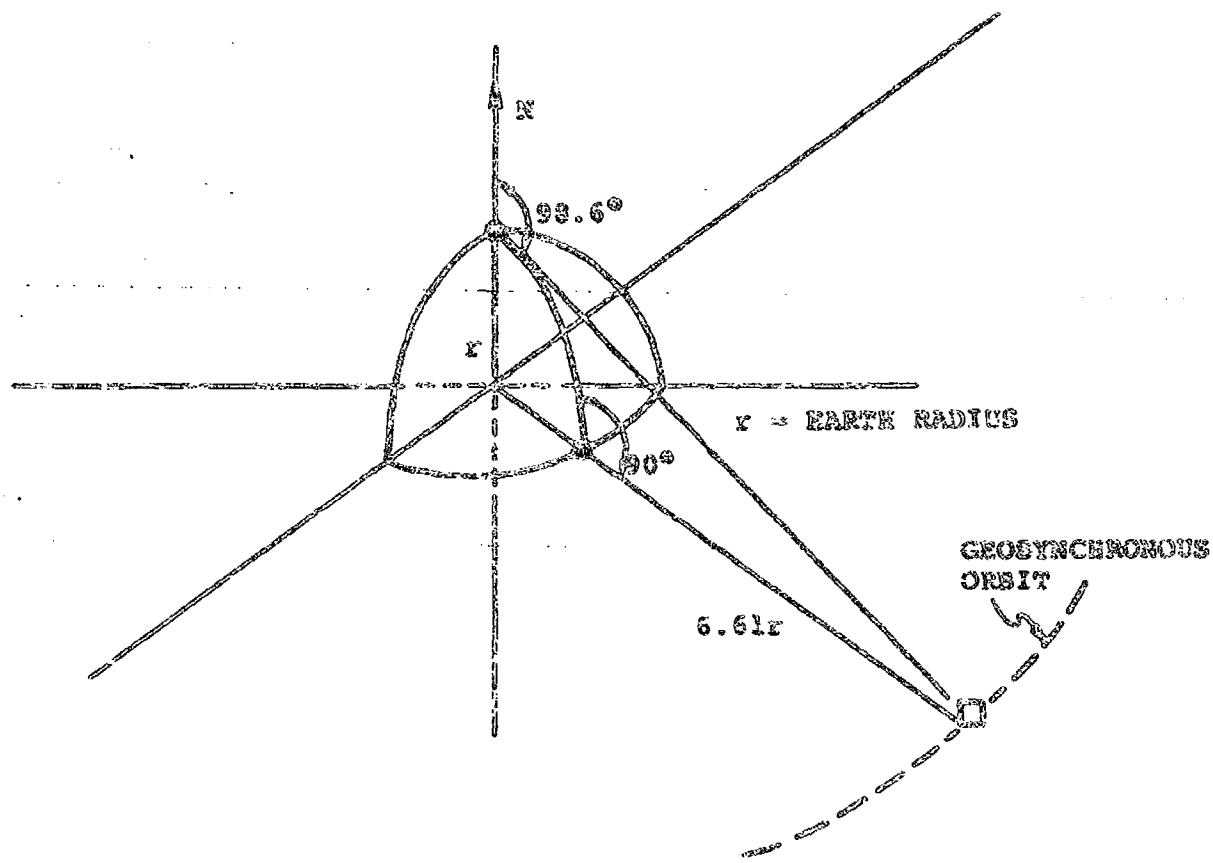


Figure 2-7. Equatorial and Polar Limits on the
Rotation Axis Angle, θ .

geostationary arc locus. A small amount of orthogonal (parabolic) plane scan is utilized to keep the MBTA beam pointing at the geostationary arc over the field of view.

The basic structural concept of the MBTA incorporates lightweight, modular, rugged, and cost-effective design. The MBTA system includes the following components:

- a. Reflector surface panels curved to a prescribed shape and a panel backup truss assembly to provide stiffness and stability. Both are universal designs independent of earth station and satellite location.
- b. Site-dependent support members to hold the reflector and truss assembly to the prescribed position.
- c. The foundation base.
- d. A separate feed tower building including the universal feed travel mechanism, which also provides an environmental and security enclosure for the communications electronics.

The components of the basic structural "package" are shown in Figure 2-8, which is a photograph of the MBTA at COMSAT Labs.

The reflector panels are relatively lightweight members with sufficient stiffness to achieve the required rms surface tolerances under operating environmental conditions. They are fabricated using conventional aluminum materials and technology to minimize cost. Adjustment mechanisms at the individual panel corners provide surface tilt corrections during assembly. The adjustment mechanism is incorporated into the panel-truss connection.

The members for the reflector truss assembly and support structure were chosen for stiffness from AISC stock steel members. This ensures that the material is readily available and allows the maximum stiffness-to-weight ratio to be selected.

Multiple Beam Torus
Antenna Study

COMSAT Labs

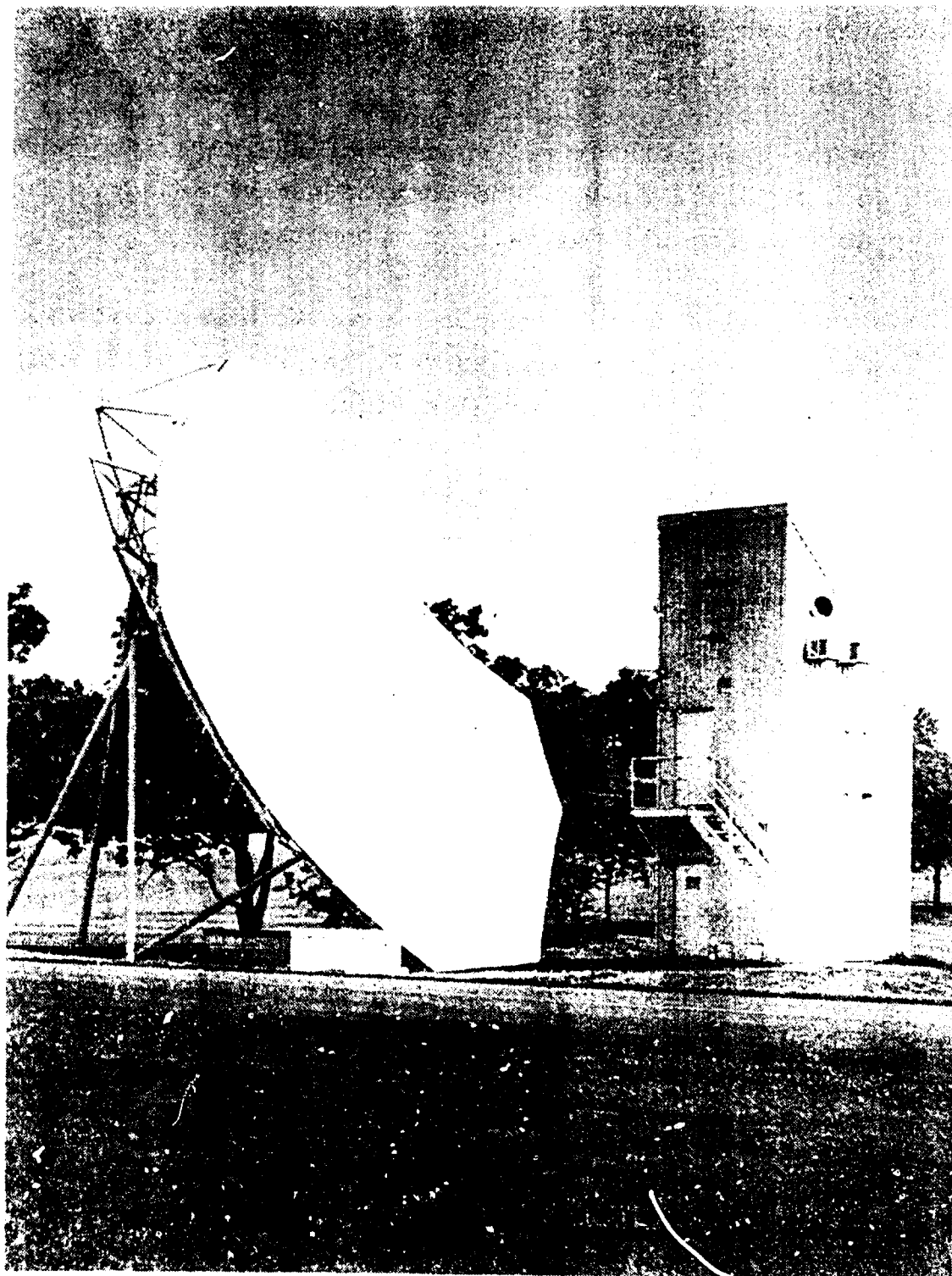


Figure 2-8. COMSAT Laboratories MBTA

The backup structure consists of a truss curved to follow the reflector surface, as shown in Figure 2-9. Several discrete points are chosen as connection points between the backup and support structures. The relative flexibility of the backup structure between connections determines the required number and location of these points.

The support structure constitutes the main load path of the antenna structure. It also provides a reflector positioning adjustment. The length of back support members is dictated by the relative earth station/satellite location. The 3-point support offers relatively little structural stiffness for even moderate size antennas. Thus, a minimum of four support points was used. For larger aperture reflectors ($D > 27$ ft) proportionally more supports would be required. The 4-point support used for the study analysis consists of a support tripod as the main static load carrying path. V- and A-frame members from the other three pickup points provide the dynamic load paths for the overturning and torsional moments. The V-frame members also provide reflector parabolic plane beam pointing adjustment. Figure 2-10 is a photograph of a similar support structure at CONSAT Labs. A typical poured-concrete foundation plan for this support layout is shown in Figure 2-11. Figure 2-12 is a back view of the reflector showing the support members and foundation pads.

A primary cost parameter is the reflector aperture area, which is a function of the basic diameter, D , and the specified field of view. Specific gain requirements fix the optimum size and curvature parameters and also specify the structural rigidity required to meet the root-mean-square (rms) surface tolerance of the reflector and feed structures and the relative beam pointing error criteria. The rms surface tolerance of the reflector is a

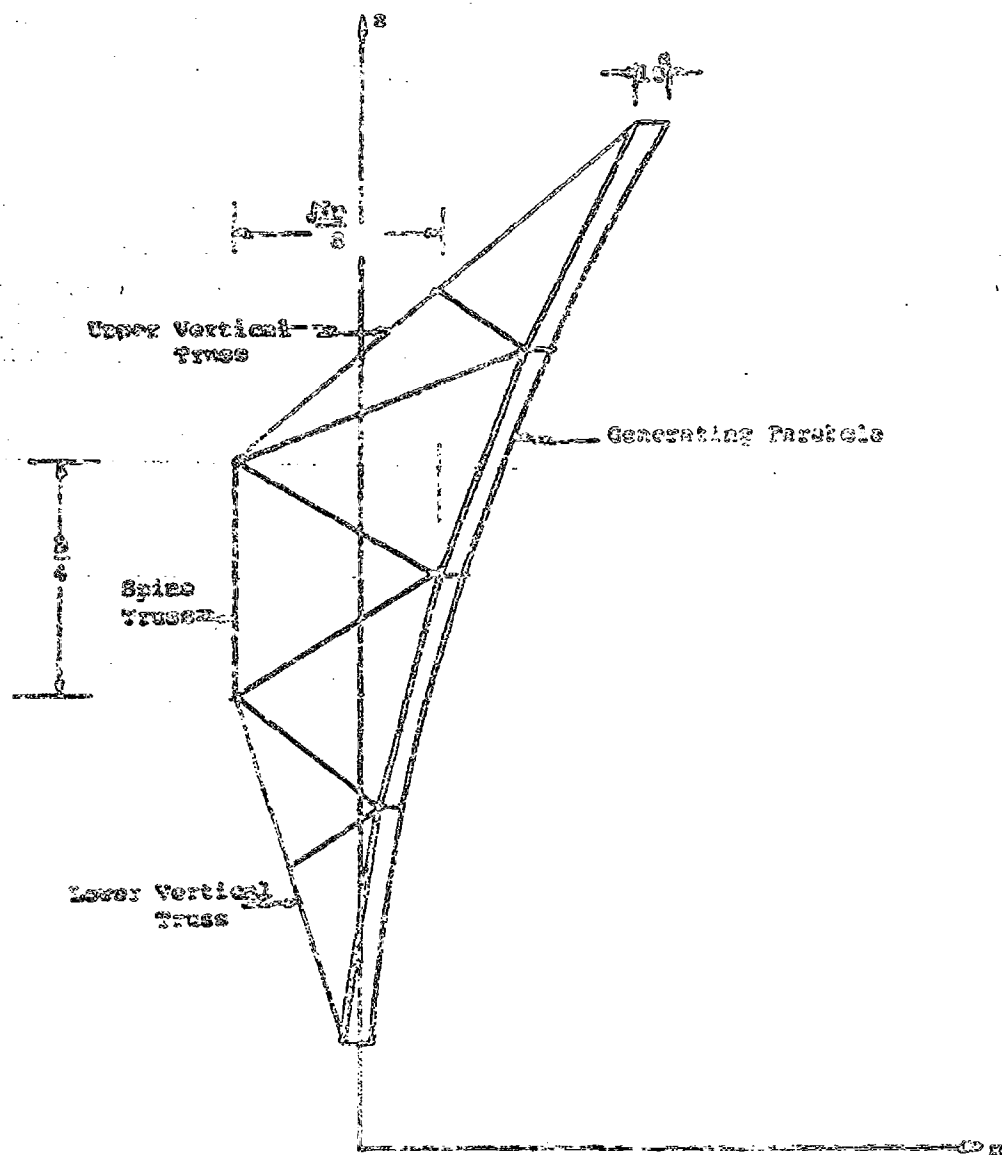


Figure 2-9. Typical 4-Panel Generating Truss

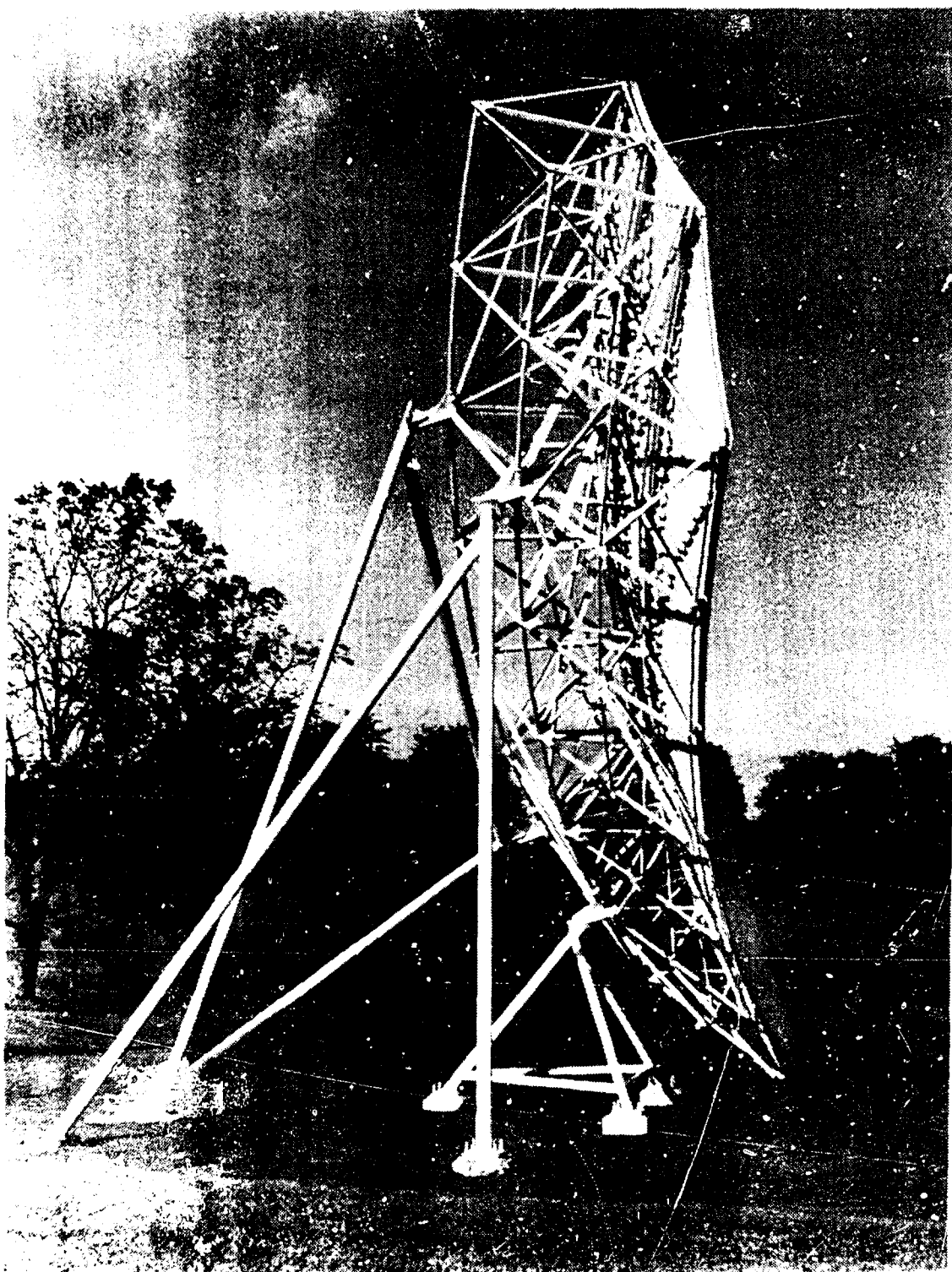


Figure 2-10. MBTA Structural Support

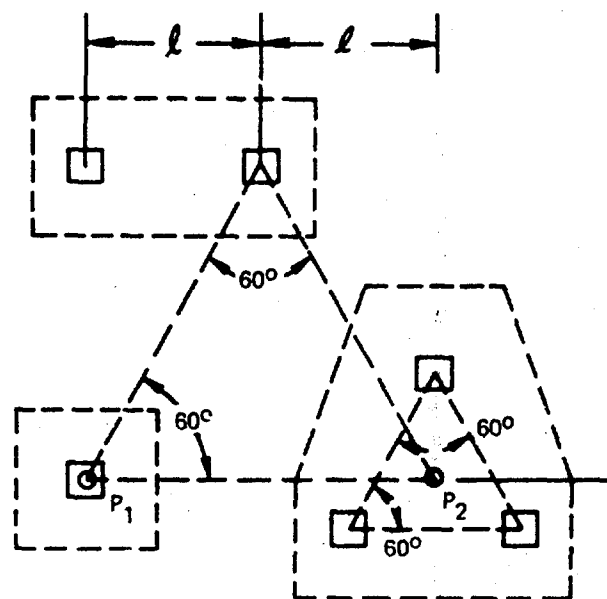


Figure 2-11. Poured-Concrete MBTA Foundation

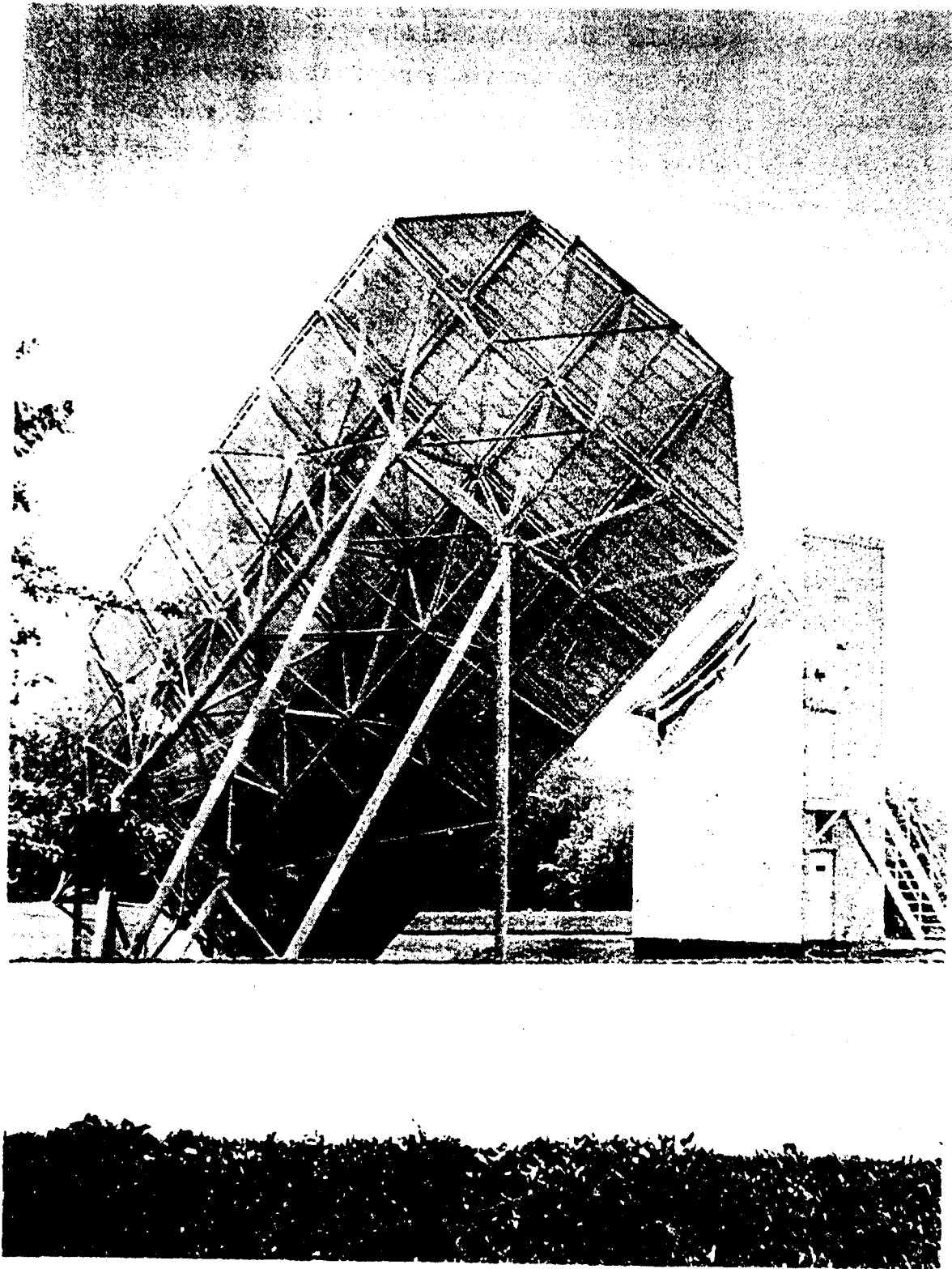


Figure 2-12. Back View of Reflector Supports
and Foundation

sum of the uncorrectable mean deviations from the best fit reflector surface. The beam pointing error is the angular difference between the original ideal reflector and the surface of the best fit reflector measured to the deflected coordinates. Figure 2-13 provides a physical definition of the rms and beam pointing errors.

The rms surface tolerance, ϵ , has a major impact on both antenna support structure requirements and cost. It is a combined function of the structural deformations due to gravity, environmental conditions, manufacturing tolerances, and rigging adjustments. Surface errors are directly related to the total reflector surface area; hence, the use of parameters to minimize the antenna size is desirable. The largest cause of pointing and surface errors is deflections due to wind forces. These forces are proportional to the projected area of the reflector on the plane perpendicular to the angle of attack of the wind and the maximum height of the antenna relative to ground.

Nearly all antenna sites project at least 60 percent of their area perpendicular to a possible wind direction. The real measure of the wind effect can be related to the moment area of the reflector. The moment area (reflector height times aperture area) relates the required panel, backup, and support structural stiffness to surface tolerances. Figure 2-14, which demonstrates the relative change of this parameter with location, shows a possible 600-percent (2.4/0.4) variation in the required stiffness of various antenna members.

The orientation of the MBTA changes with the relative earth station location, as shown in Figure 2-15. The most difficult reflector support requirements are associated with antenna locations at low latitudes ($<40^\circ$) and at maximum relative longitude differences. The reflector height above ground and its exposed area are then maxima. The most difficult feed tower

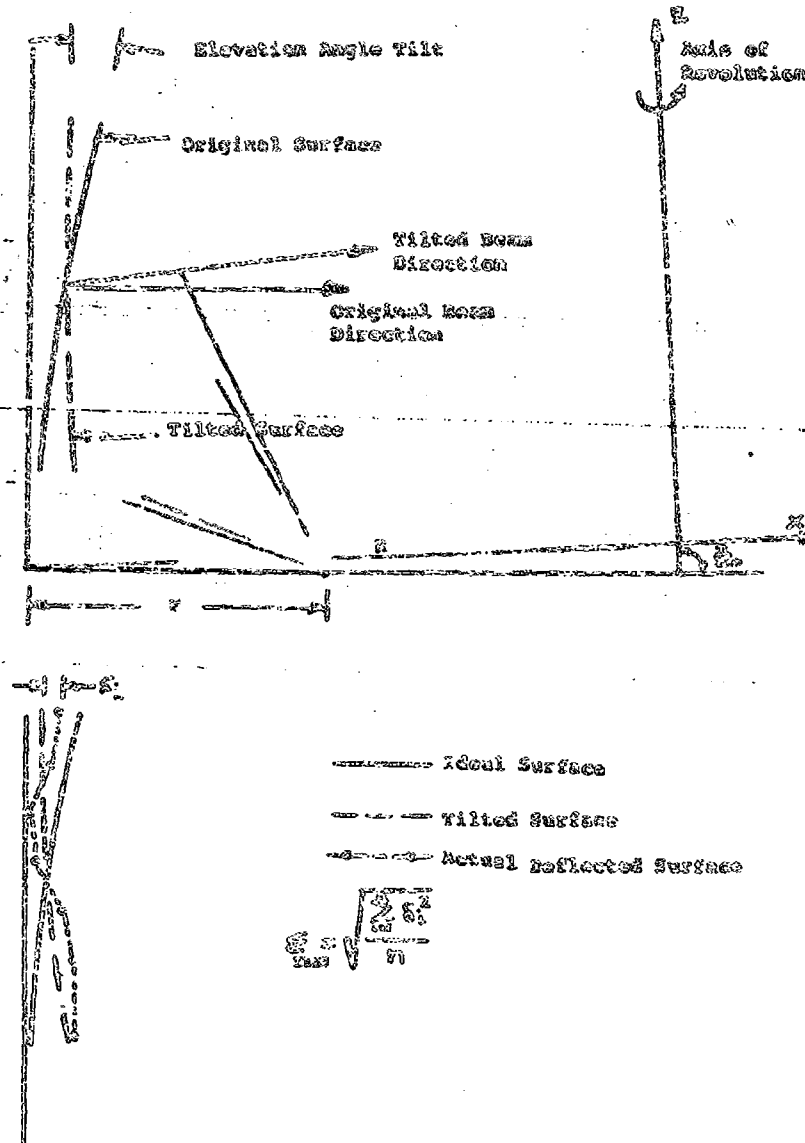


Figure 2-13. Beam Pointing and rms Surface Errors

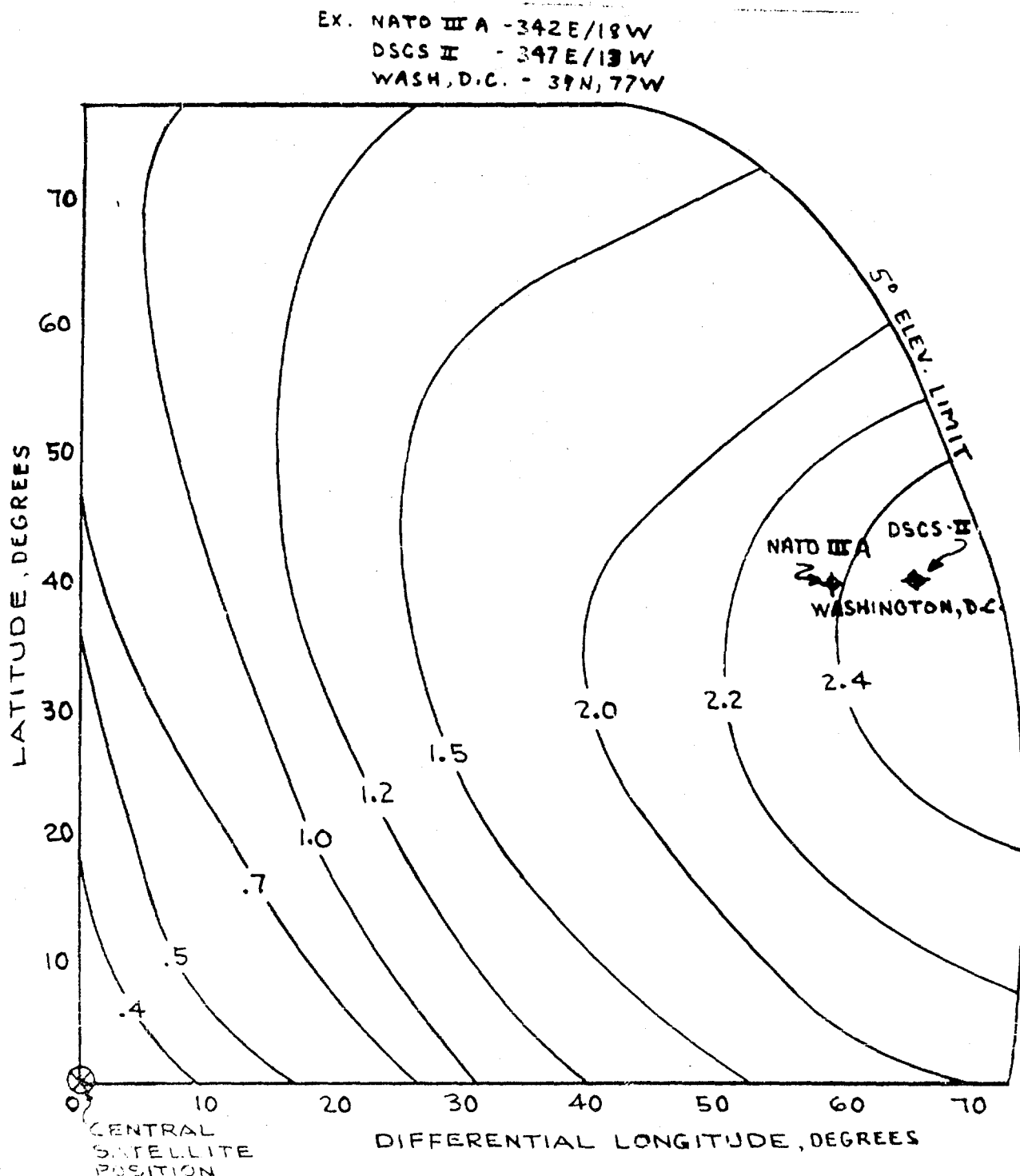
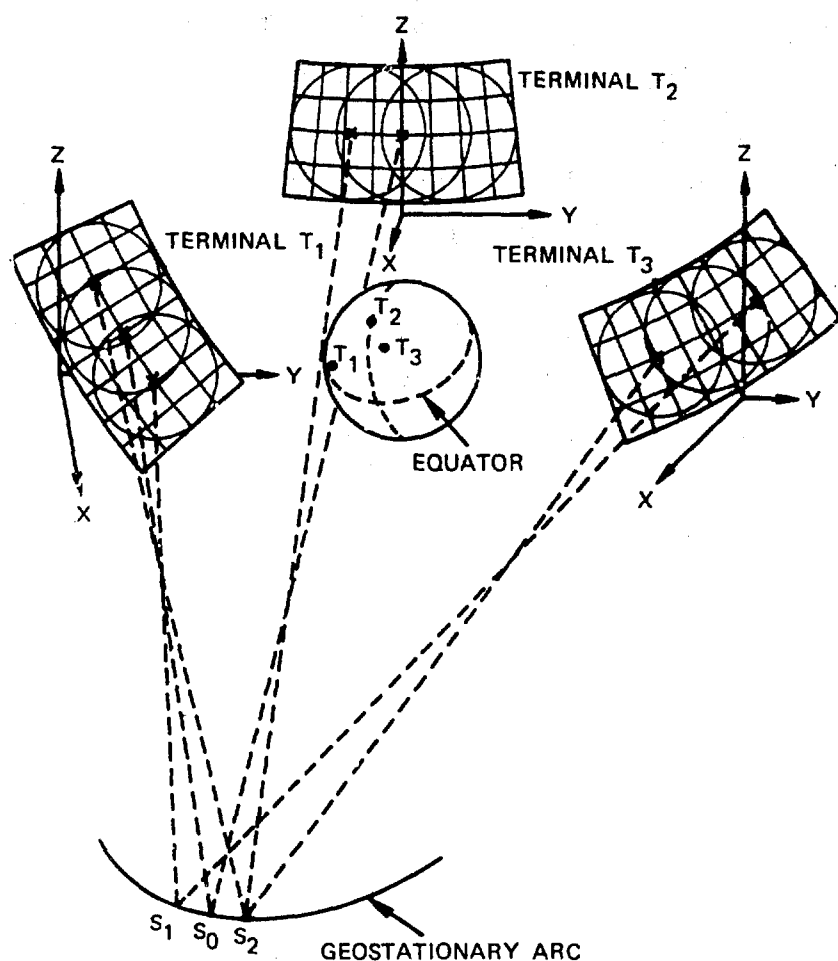


Figure 2-14. Normalized Wind Moment Area $[(A \cdot H) / (W \cdot D^2)]$



s_0 = CENTRAL SATELLITE AT 333° EAST LONGITUDE
 λ = LATITUDE LOCATION OF TERMINAL
 l = LONGITUDE LOCATION OF TERMINAL
 ξ = ANGLE OF ELEVATION AT SITE
 Ω = ANGLE OF TILT AT SITE
 z = LOCAL VERTICAL AT SITE
 xy = GROUND PLANE AT SITE

	λ	l	ξ	Ω
T_1	27N	279E	23	57 0
T_2	70N	333E	11	0
T_3	47N	11E	24	28

Figure 2-15. MBTA Orientation at Different Earth Locations

structure requirements occur for an antenna located at the sub-satellite point (latitude = 0; longitude difference, λ = 0) and along the equator. The feed tower height and width are then maxima.

The principal mechanical objective has been to design a simple, reliable, lightweight, and semi-transportable MBTA structure which can be utilized at the majority of antenna locations in a widely deployed DSCS system. Common structural support systems and feed housing are used for different antenna locations. The dimensions of structural members and panels are chosen to simplify the transport and erection of the MBTA.

3. SUMMARY OF MAJOR STUDY RESULTS AND GENERAL RECOMMENDATIONS

The primary advantages of the fixed reflector, offset-fed MBTA for geosynchronous satellite applications are as follows:

- a. exceptional RF performance in critical areas, particularly sidelobes and multifrequency operation;
- b. simplicity and reliability; and
- c. cost savings in multiple-beam and/or multiple-frequency-band applications.

This section summarizes the major study results and recommendations concerning the applicability of the MBTA to the NSCS communications requirements and describes the performance advantages.

3.1 RF PERFORMANCE

This study focuses on the analysis and evaluation of medium-gain MBTA configurations providing 54-59 dB of receive band gain at the government X-band frequencies (7.25-7.75 GHz receive, 7.9-8.4 GHz transmit). However, overall antenna system performance is evaluated for frequencies ranging from 3.7 to 31 GHz to ascertain the multi-frequency-band capabilities of the MBTA in the following bands:

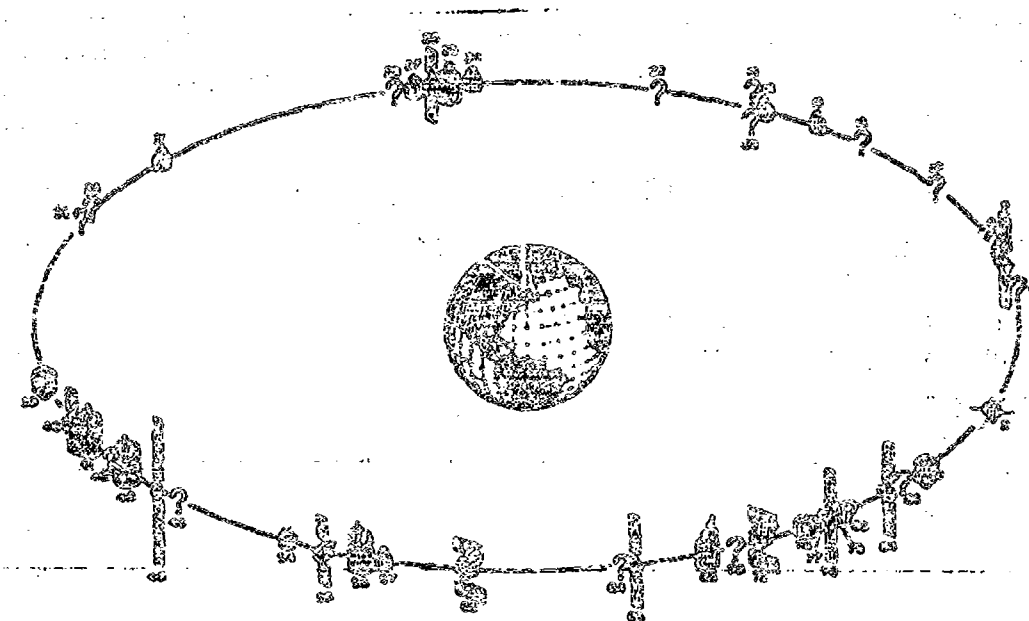
- a. C-band (commercial frequencies of 3.7-4.2 GHz receive, 5.925-6.425 GHz transmit),
- b. 11/14 GHz (commercial frequencies of 10.95-11.2 and 11.45-11.7 GHz receive, 14.0-14.5 GHz transmit, and 11.7-12.2 GHz), and

c. X-band (20.2-21.2 GHz receive, 30-31 GHz transmit).

An offset geometry provides an unblocked antenna aperture plane (feed, subreflector, or spars) and eliminates forward feed spillover (Cassegrain geometries), thus providing the basis for realizing low wide-angle sidelobe pattern characteristics. The sidelobe characteristics of earth station antennas have become a critical performance factor as the number of communications satellites and terrestrial systems increases and interference restrictions become more stringent. Therefore, the implementation of offset MOTA geometries rather than symmetrical geometries is recommended even though the aperture efficiency is somewhat reduced. Figure 3-1 shows the number of geosynchronous satellites launched or to be launched after January 1, 1976.

The basic relationships between antenna gain and beamwidth as a function of the circular aperture diameter/wavelength ratio (D/λ) of a reference parabolic reflector are given in Figure 3-2. Aperture illumination efficiencies of $\eta = 65$ percent represent a reasonable but stringent design goal, particularly for antenna systems which require good sidelobe characteristics. Feed system and rms surface tolerance losses must be added to the aperture illumination efficiencies to obtain the overall antenna system gain for each D/λ value.

The illumination gain of the offset MOTA fed with a single feed at the parabolic focus is presented in Figure 3-3 as a function of D/λ . Spherical aberration phase errors associated with the MOTA geometry increase directly with D/λ . Maximum gain is realized by reducing the illuminated aperture area relative to the physical aperture after a critical D/λ value is reached on each D/λ curve. This value of D/λ occurs when the illumination gain is reduced by 3.5 to 4.0 dB relative to a 100-percent



KEY:

1	NEOSAT	43	SBS-A
2	GOES	45	COMSTAR-A
3	STATSIONAR 2	46	CTS
5	MAROTS	49	SBS-B
6	STATSIONAR	50	NES-A
9, 10	STATSIONAR 5	55	NATCOM-C
13	FUTURE METEOROLOGICAL SATELLITE	56	CURSTAR-C
16	PALAPA-2	57	NBS-B
18	PALAPA	61	PLTSATCOM
19	STATSIONAR 3	64	TOSS
20	STATSIONAR 6	65	AEROSAT
22	STATSIONAR 7	68	INTELSAT IV-A F2
24	IRIA IX	70	STATSIONAR 8
25	CS	72	PLTSATCOM
26	RS	76	NATO-3
27	GOES	77	SIRIO
28	STATSIONAR 7	78	AEROSAT
31	MARISAT	79	MARISAT
35	SDRS	80	STATSIONAR 9
36	STATSIONAR 10	84	OTS
39	FUTURE SRS	85	TV BROADCAST
40	SATCOM-B		
41	COMSTAR		

Figure 3-1. Geosynchronous Satellites Launched
or to be Launched after January 1, 1976

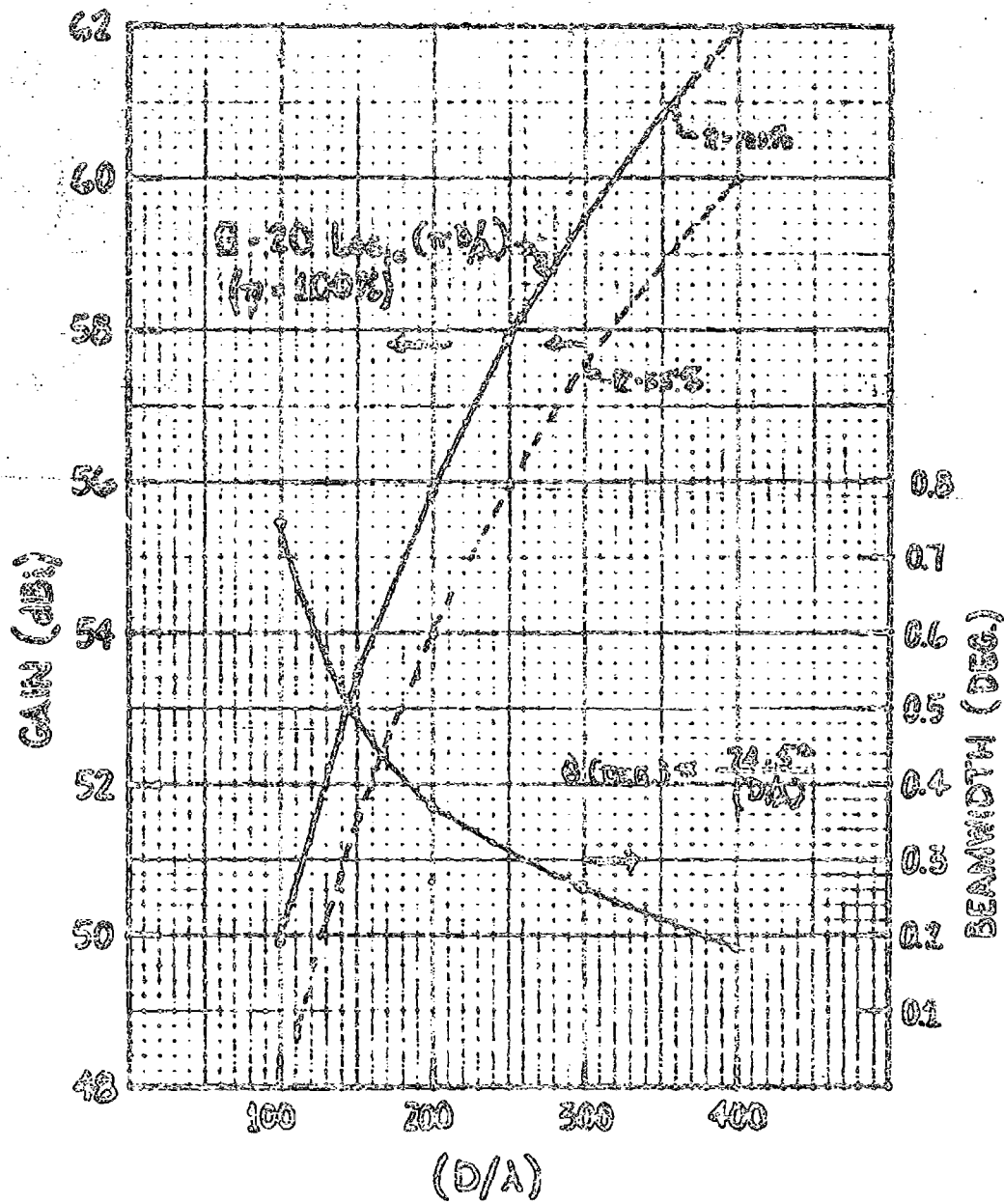


Figure 3-2. Illumination Gain and Beamwidth versus D/A
of a Parabolic Reflector

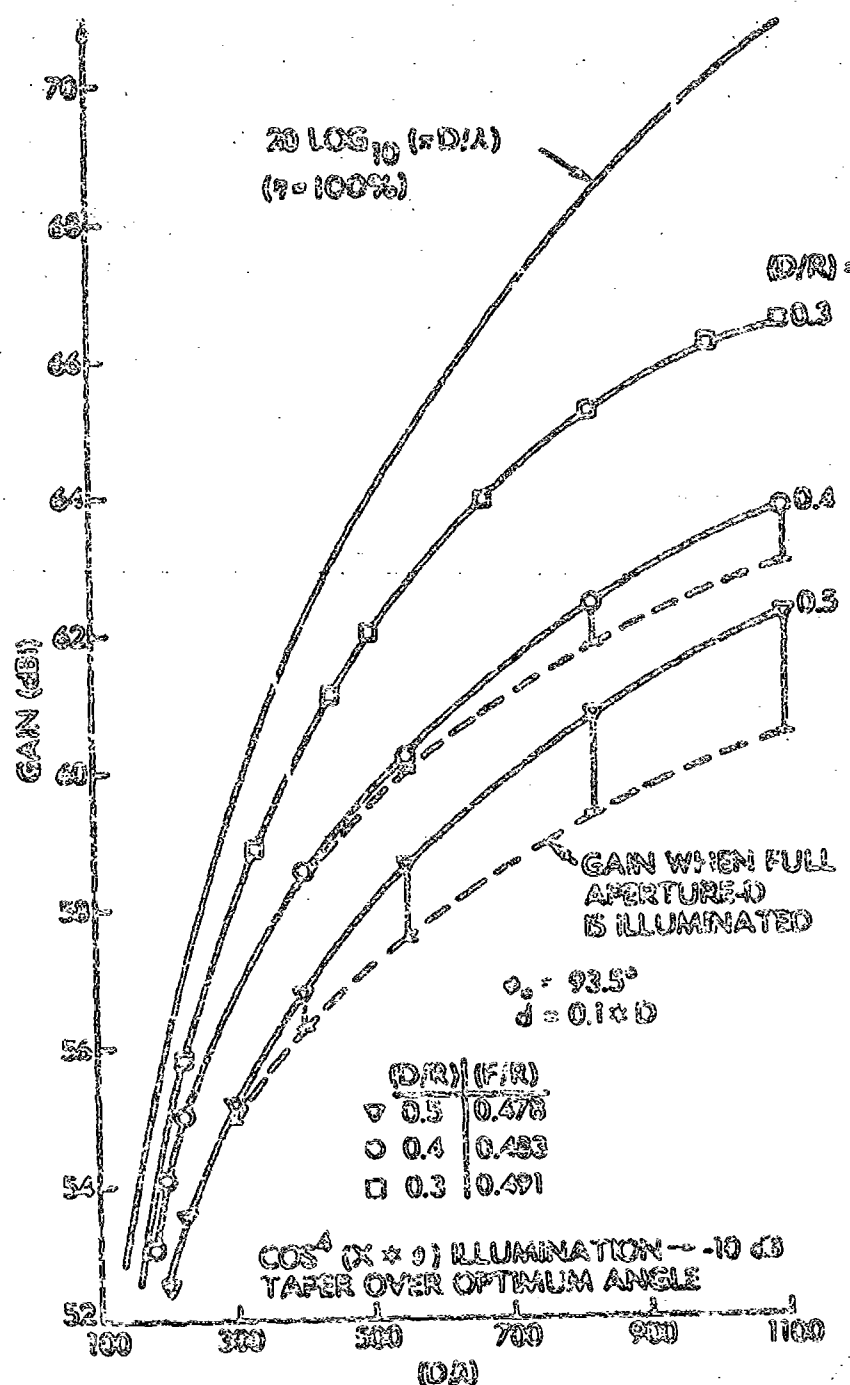


Figure 3-3. Illumination gain of offset HBTX versus D/A with fixed radius of curvature $(D/2)^{-1}$

efficient physical aperture gain. For the $D/R = 0.3$ geometry, the illumination efficiency remains above 65 percent for D/λ values up to 600 ($G \approx 63$ dB) and above 50 percent for D/λ values up to 800 ($G \approx 65$ dB).

Figure 3-4 shows diameter vs D/λ for minimum down-link frequencies and maximum up-link frequencies over the frequency bands of interest in this study program.

The gain loss of the antenna system associated with rms surface tolerance (ϵ) losses is shown in Figure 3-5. The rms surface tolerance has a major impact on the multi-frequency-band operation of the MBTA and the antenna support structure requirements, panel fabrication, and cost. Because surface tolerance losses and spherical aberration effects are both frequency dependent, the "optimum" antenna design is also frequency dependent.

In addition to the surface tolerance, the required field of view of the MBTA has a major impact on the mechanical and structural requirements. Figure 3-6 shows the field of view versus the ratio of aperture dimensions (W/D) for particular D/R values. For a fixed field of view requirement, W/D increases as the radius of curvature is increased (D/R decreases) to reduce spherical aberration effects.

The minimum spacing between adjacent beams along the geostationary arc, which is constrained by the physical diameter of the feed horn aperture, d_h , is

$$\Delta\theta_{\min} = \frac{(360^\circ/\pi)(D/R)(d_h/\lambda)}{(D/\lambda)} \quad (3-1)$$

which is approximately 2-4 antenna half-power beamwidths depending upon the type of feed horn used. Thus, for the two X-band antenna systems considered,

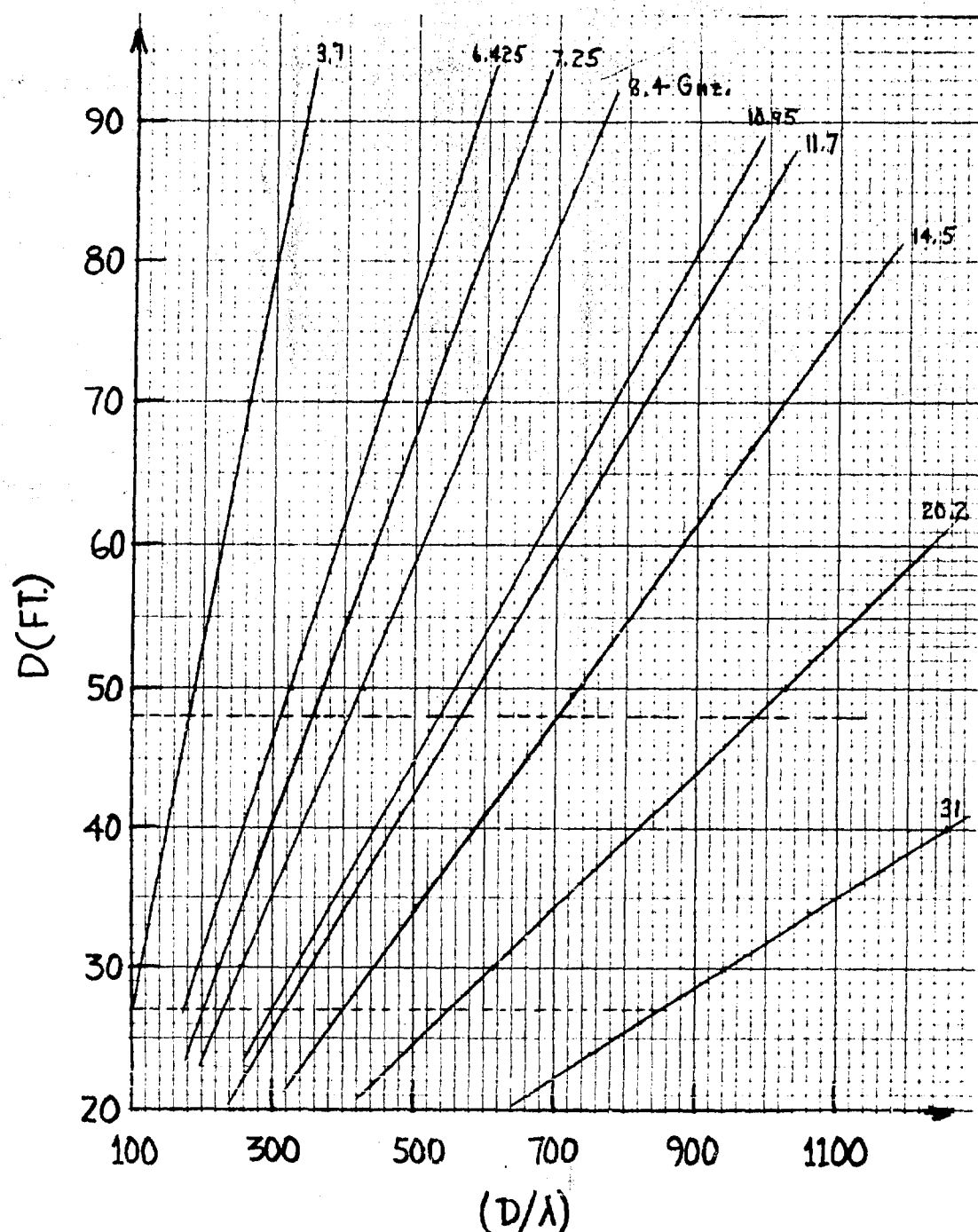


Figure 3-4. Diameter, D , versus D/λ for Minimum Down-Link and Maximum Up-Link Frequencies

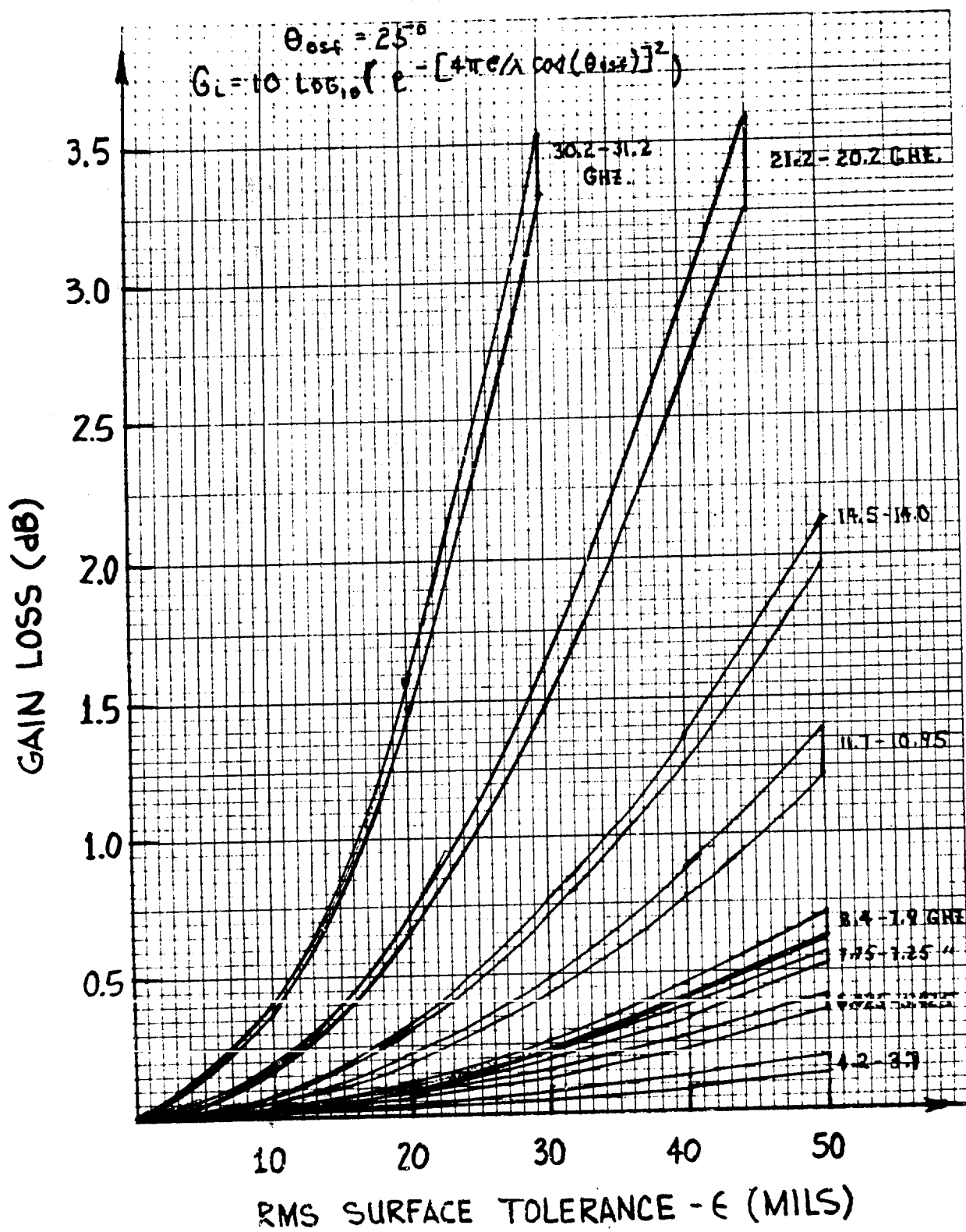


Figure 5. MBTA Surface Tolerance Gain Losses

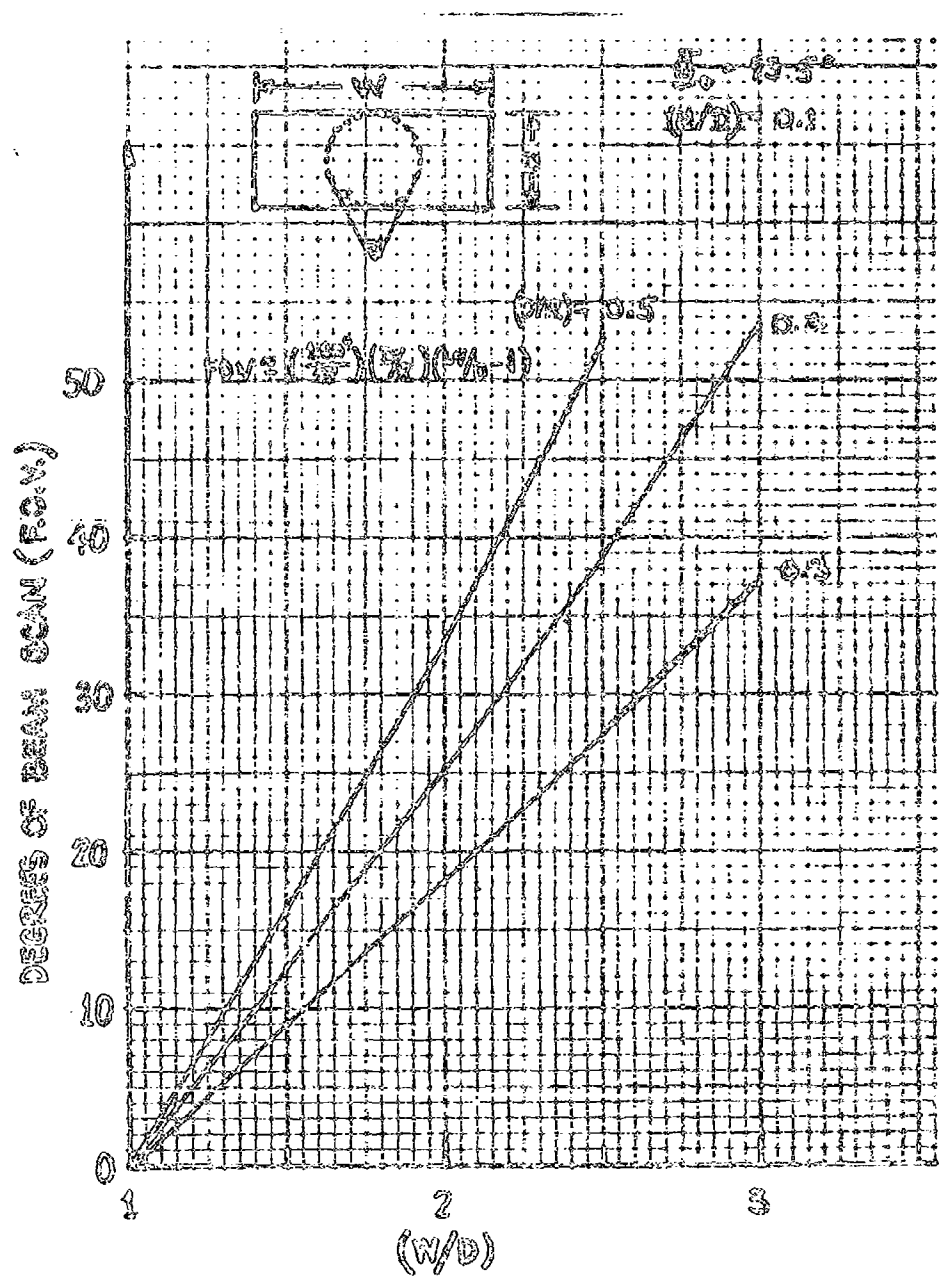


Figure 3-6. MBTA Field of View (FOV) versus the Ratio of Aperture Plane Dimensions, W/D

$$G = 54 \text{ dB for } \Delta\theta_{\min} \approx 1.2^\circ \quad (3-2a)$$

$$G = 59 \text{ dB for } \Delta\theta_{\min} \approx 0.8^\circ \quad (3-2b)$$

The antenna noise temperature profile for the MBTA at X-band as a function of elevation angle is shown in Figure 3-7. The absence of aperture plane blockage and scattering and the use of an oversized reflecting surface for multiple beam formation result in exceptional antenna noise temperature profiles for the offset MBTA.

Figures 3-2 to 3-7 form the basis for defining the RF performance characteristics of the MBTA system. The system designer must specify a required set of gains (or G/T) and frequency bands, and a required field of view. These specifications in turn permit a tradeoff among D (or D/ λ), D/R, W/D, and ϵ parameters, which in turn can be normalized to a cost/performance relationship.

The gain performance of the offset MBTA over the range of 3.7 to 31 GHz is indicated in Figure 3-8, which shows the aperture illumination gain of a 27-ft-diameter antenna. With a specified X-band gain requirement of 54 dB and a 30° field of view, the D/R = 0.4 configuration provides an "optimum" compact geometry (W/D = 2.20). However, in the 20/30-GHz frequency bands the illumination gain of the D/R = 0.4 configuration is ~2.3 dB lower than that of the D/R = 0.3 geometry. If 52-dB antenna system gain is required at 20 GHz, then the D/R = 0.3 geometry with its associated larger aperture area (W/D = 2.65) is necessary.

The patterns of the 27-ft-diameter MBTA with D/R = 0.4 are shown in Figures 3-9 and 3-10 for the government X-band frequencies. These patterns are calculated at the mid-band

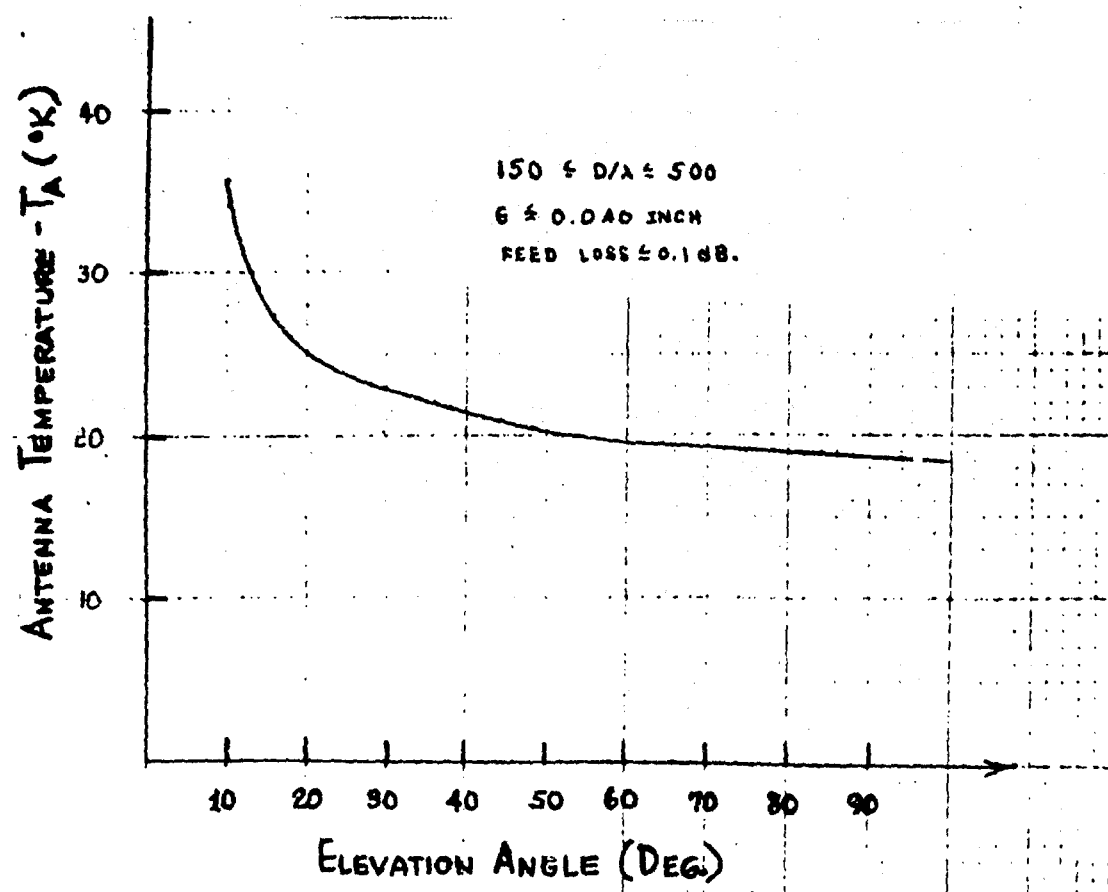


Figure 3-7. MBTA Antenna Noise Temperature at X-Band

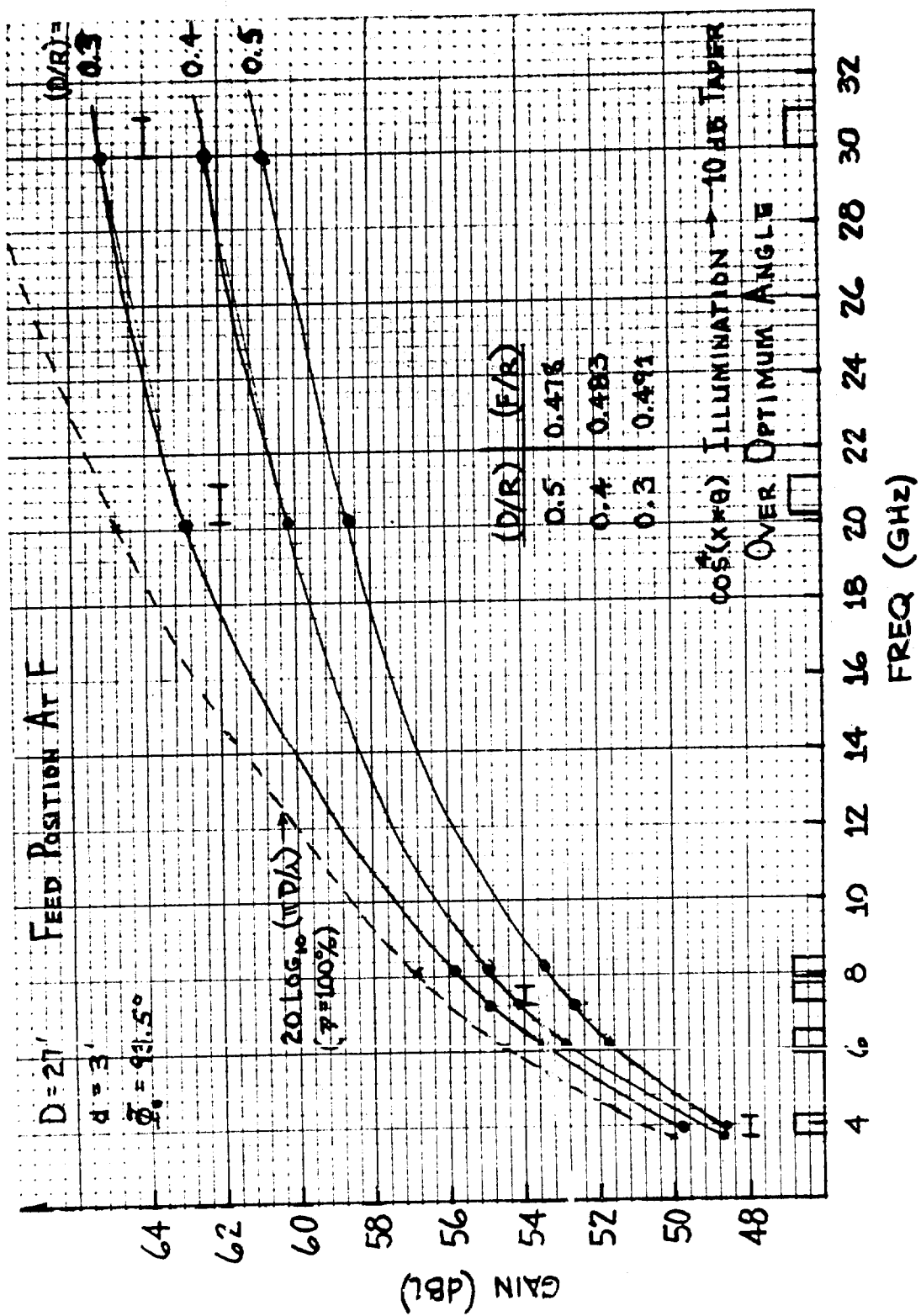


Figure 3-8. Baseline MBTA ($D/R = 0.4$) Illumination Gain from 3.7-31 GHz

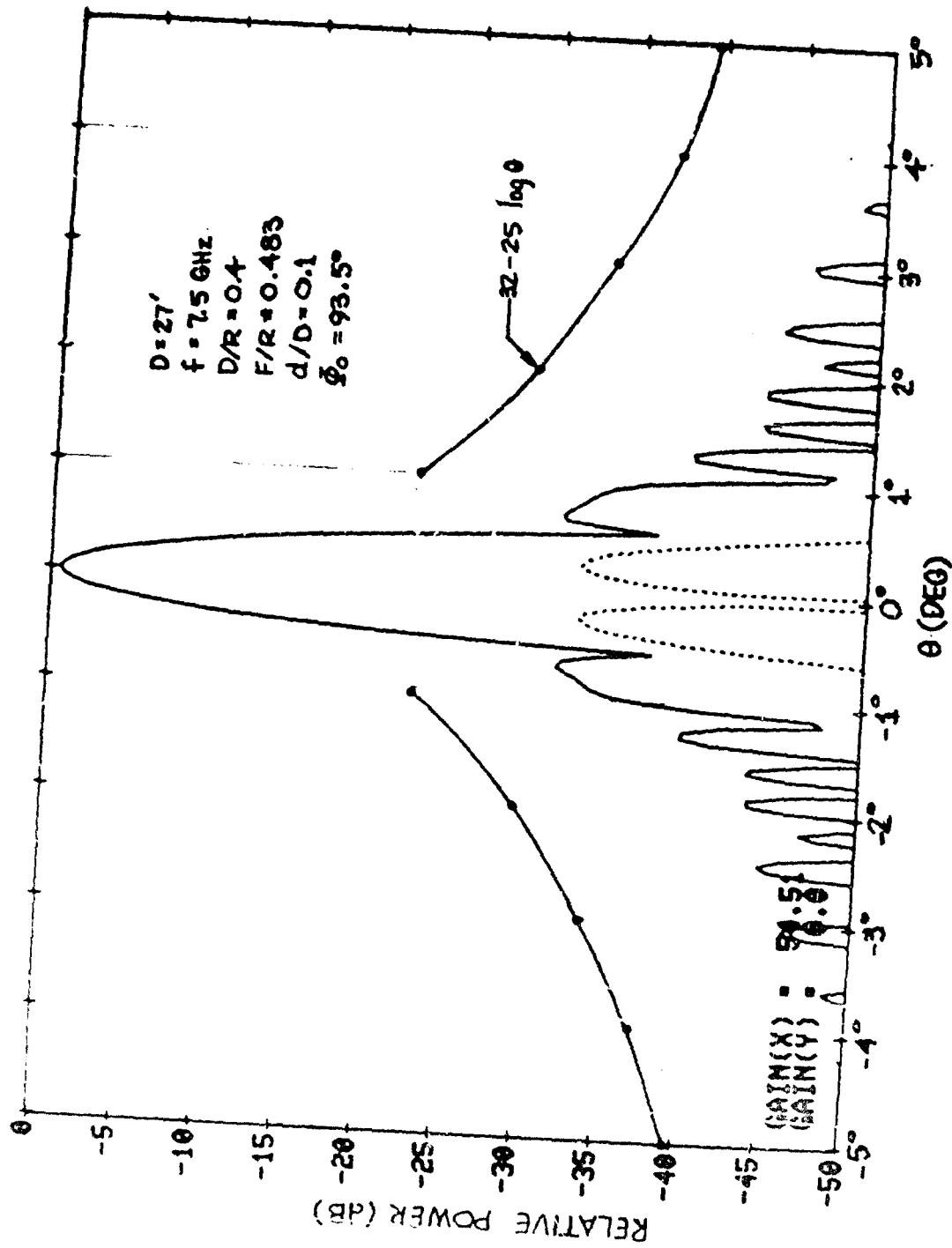


Figure 3-9. Baseline 27-ft-Diameter MBTA Pattern at 7.5 GHz ($\phi = 90^\circ$)

Multiple Beam Torus
Antenna Study

COMSAT Labs

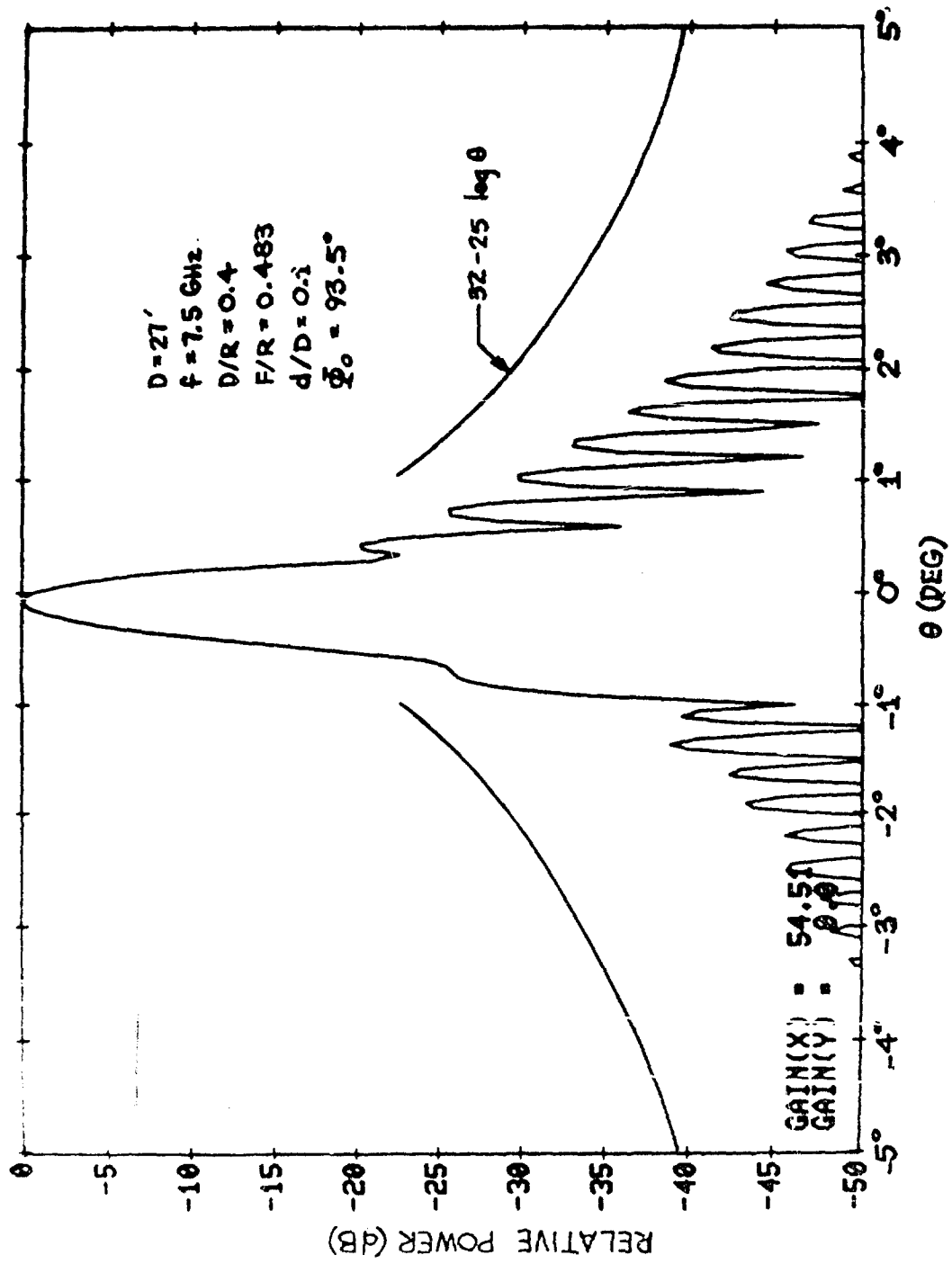


Figure 3-10. Baseline 27-ft-Diameter MBTA Pattern at 7.5 GHz ($\phi = 0^\circ$)

receive frequency of 7.5 GHz. For reference the 32 - 25 deg., 6 performance requirement for conventional antennas is given as a dashed line. The first pattern ($\phi = 90^\circ$), which is in the scan plane (along the geostationary arc), demonstrates the excellent sidelobe characteristics of the offset MBTA. The second pattern is in the plane containing the parabolic section of the MBTA. The offset asymmetry combined with spherical aberration gives rise to a minor sidelobe asymmetry and beam squint. The half-power beamwidths in the spherical and parabolic planes are 0.36° and 0.34° , respectively.

As shown in Figure 3-11, 59-dB receive band gain is realized with a 48-ft-diameter offset MBTA ($D/R = 0.3$) at the government X-band frequencies. The aperture illumination efficiency, $\eta = 70$ percent. The $D/R = 0.4$ geometry with $D = 48$ ft., realizes an aperture efficiency of $\eta = 47$ percent at X-band. A 59-dB gain requirement at X-band combined with a multifrequency performance capability from 3.7-31 GHz would clearly favor the $D/R = 0.3$ geometry. The full aperture diameter, D , is utilized over the entire frequency range. With the $D/R = 0.4$ geometry, the illuminated aperture area of the antenna system must be reduced relative to the physical aperture to realize optimum gain in the 11/14- and 20/30-GHz bands. A smaller field of view for the 59-dB-gain antenna system can be utilized to constrain its W dimension.

The MBTA geometry provides a conical beam scan locus which closely approximates the curvature of the geostationary arc when the parabolic generating curve and feed position are revolved about the rotation axis, u . For geosynchronous applications, the optimal generating axis angle, θ_0 , varies from 90° for MBTAs located at the equator to 98.6° for those close to the polar regions.

A single reflector design defined as

$$\theta_0 = 93.5^\circ \quad (3-3)$$

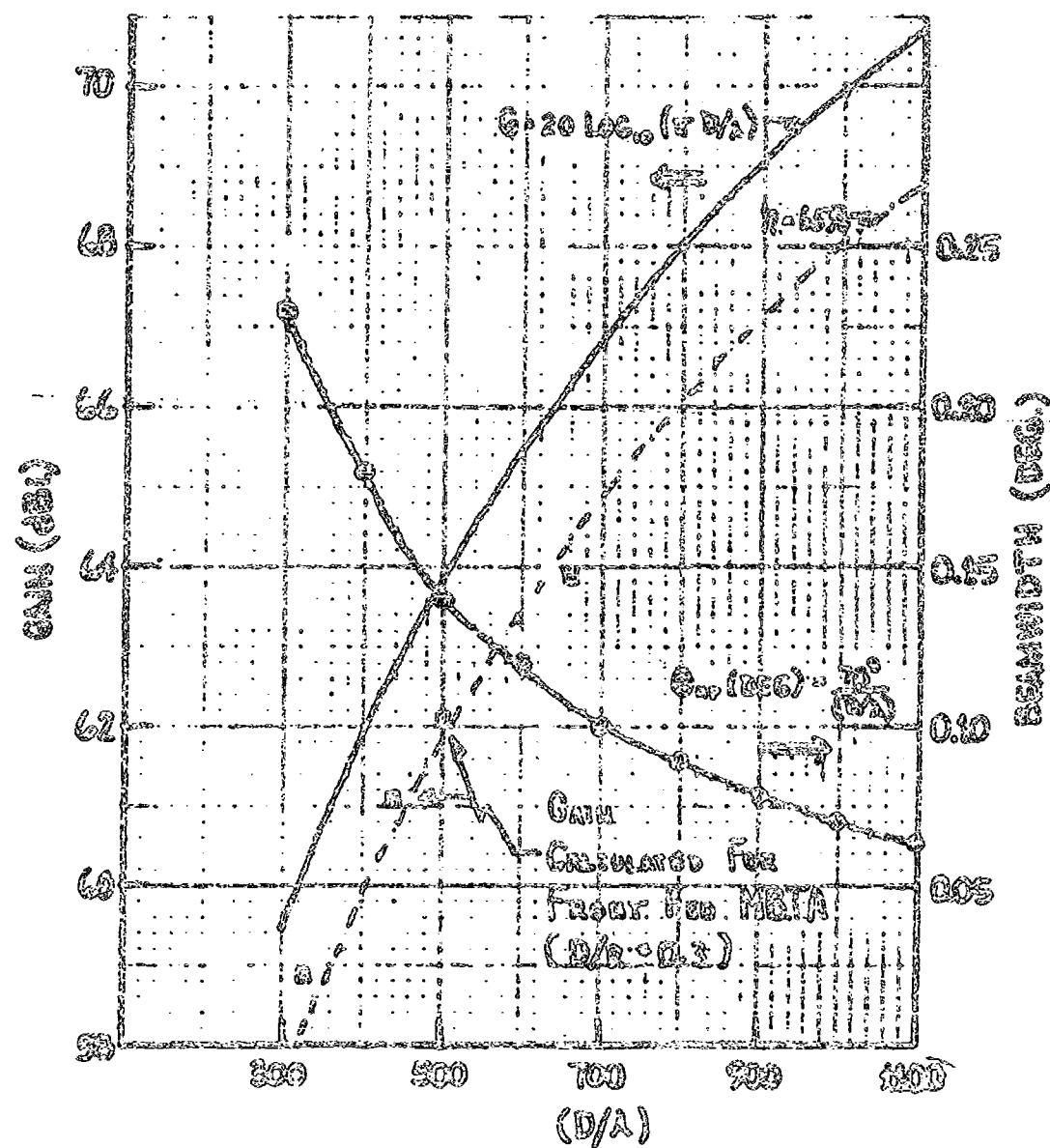


Figure 3-11. Aperture Illumination Gain and Beamwidth versus D/λ for $D/R = 0.3$ MSTA Geometry

is sufficient for a widely deployed earth station antenna system and results in less than 0.3° of worst-case beam pointing error with spherical plane scan over a 40° field of view, as shown in Figure 3-12 for a specified set of NSPA locations. This beam scan error represents less than 1-2 beamwidths of required parabolic plane scan for exact beam repositioning in NSPA having 54- to 59-dB gain; therefore, it has negligible impact on RF performance. One identical reflector surface is utilized at all NSPA locations for a given gain requirement to minimize reflector fabrication costs. The reflector support structure lengths vary to accommodate different NSPA latitudes and longitudes. The beam scan error shown in Figure 3-12 can be halved by adjusting (biasing) the antenna mount at each latitude to provide two exact scanned beam positions over the field of view. The NSPA field of view is related to the ratio of aperture plane dimensions (W/D) as follows:

$$\text{fov} = \left(\frac{180^\circ}{\pi} \right) (D/R) (W/D - 1) \quad (3-6)$$

Measurement results at COMSAT Laboratories have demonstrated that the radiation isolation between adjacent beams is precisely that predicted by the sidelobe envelopes. Direct interaction between corrugated feed horn elements is exceptionally low due to the highly tapered aperture field distributions and the absence of coupling currents on the exterior walls of these horns. The radial feed arc which tends to point the feeds away from each other also helps to minimize direct beam-to-beam coupling.

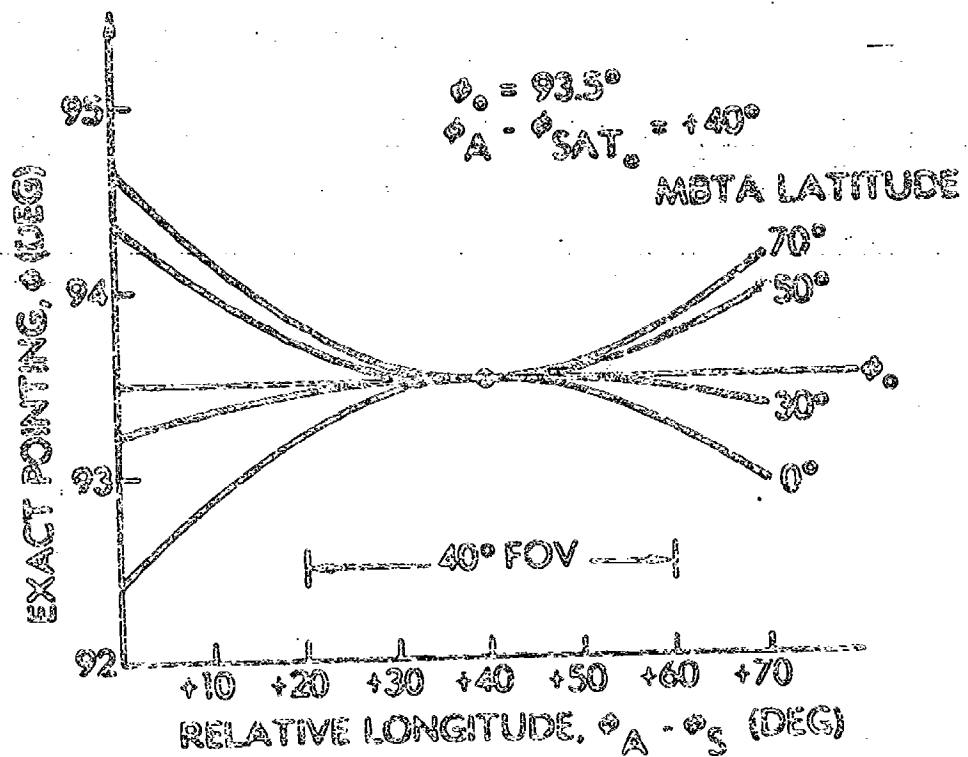


Figure 3-12. Single Reflector ($\theta_0 = 93.5^\circ$) NBPA
Pointing Error with Spherical Scan

3.2

STRUCTURAL, MECHANICAL, AND COST CONSIDERATIONS

The baseline NSRA identified in this study provides 34-dB receive X-band gain over a 30° field of view. The parameters for the baseline geometry are as follows:

$$\begin{aligned}D &= 27 \text{ ft} \\W &= 63 \text{ ft } (\text{FOV} = 30^\circ) \\D/R &= 0.4 \\R &= 67.5 \text{ ft} \\q_1 &= 93.3^\circ \\2\phi &= 62^\circ \\q_{\text{off}} &= 27^\circ \\P/R &= 3.483\end{aligned}$$

A backup truss and support structure required to realize operational rms surface tolerances of 0.040 inch (1 mm) and 0.020 inch (0.5 mm) were analyzed. The 0.040-inch rms surface tolerance represents an upper bound for acceptable RF performance at X-band. The gain loss is 0.5 dB, as shown in Figure 3-5. However, gain losses in the higher frequency bands, particularly 20/30 GHz, are excessive. The 0.020-inch rms surface tolerance results in less than 0.15-dB gain loss at X-band, and reasonable efficiencies are maintained in the 20/30-GHz bands (i.e., 1.5-dB gain loss at 30 GHz). Overall surface tolerances better than 0.020 inch result in unacceptably heavy and massive support structures. The choice of the rms surface tolerance actually implemented depends upon the intended use of the NSRA in the 11/14- and 20/30-GHz bands.

The mechanical design specifications listed in Table 3-1 describe the environmental and thermal conditions considered for the baseline NSRA during the study. The mechanical design results

Multi-Beam Beam
Antenna Study

COMMITTEE

Table 2-1. Outlines of Multi-Beam Beam Antenna Specifications

Designator	Defined Antennas	Design Antennas
Size	Overall (W x D) Panel 1, 6 ft x 12 in	60 in 27 ft (18 x 9 in) 7.3 x 7.9 ft (2.2 x 2.4 m)
Materials		A36 Steel 350 Steel Brazed-formax aluminum over a laminated basswood plywood core stainless concrete
Support		10 tons assembled
Panel 1	Minimum dimension less than 6 ft x 12 in	Size or 1000 ft long board
Panel 2		Wind load
Dimensions		Minimum dimension 12 x 1.2 x 1.2 ft to accommodate crane port, mechanism, equip- ment, etc.
Weight		
Panel Building		
Environment		Environmental Condition
Volume		
Operations	30-day window (grain 60 45 mph)	45 days (72 km/hr)
Storage	45-day window (grain 60 60 mph)	60 days (97 km/hr)
Observations	60 mph	125 mph (200 km/hr)
Survival		
Materials		
Antennae Temperature	-45°F (-37°C) to 125°F (52°C)	10°F (5.5°C)
Differential Temperature	10°F (5.5°C)	

TABLE 3-2. OUTLINES OF INTRA MECHANICAL SIGNALS (CONTINUED)

PARAMETER	DIRECT SIGNALIZATION		SPLIT SIGNALIZATION	
	ENVIRONMENTAL DATA (CONTINUED)		ENVIRONMENTAL DATA (CONTINUED)	
RFID DIRECT SIGNALIZATION				
Frequency = 7.25 GHz.				
Gain = 94 dB				
Operational (-0.5 dB)	0.040 in.		0.040 in. (1 cm)	
Degraded Operational (-1 dB)	0.040 in.		0.060 in. (1.3 cm)	
RFID SPLIT SIGNALIZATION				
Frequency = 20.2 GHz.				
Gain = 62 dB				
Operational (-0.5 dB)	0.018 in.		0.020 in. (0.5 cm)	
Degraded Operational (-1 dB)	0.025 in.			
RFID DIRECT SIGNALIZATION				
Frequency = 30 GHz.				
Gain = 64 dB				
Operational	0.012 in.		0.020 in. (0.5 cm)	
Degraded Operational	0.017 in.			

COMMITTEE

Multiple Beam Torus
Antenna Study

in a simple, lightweight, transportable structure permitting worldwide MBTA deployment. The reflector panel surface and backup truss support structure are identical for all site locations. The length of the A- and V-frame structural support members are varied to accommodate different MBTA locations. The reflector panels and backup truss structure are designed to facilitate commercial fabrication and handling and shipping of individual members.

Several representative antenna locations shown in Figure 3-13 were selected to evaluate the effect of worldwide deployment on the basic antenna structure. The satellite location is a middle location for the LES-9, NLTSATCOM, NATO-II, NATO-III, and DSCS satellite arc. Figures 3-14 and 3-15 are views of the baseline MBTA antenna system at four different locations, indicating the variation in MBTA geometry.

The feed tower height and window slope vary considerably as a function of relative antenna location, as shown in Figures 3-14 and 3-15. Figure 3-16 shows the product (area) of feed tower width times maximum height. A single feed transport (radial rail) assembly is utilized for all MBTA locations. The feed transport arc length, as shown in Figure 3-17, is a function of D/R, P/R, ϕ , and FOV, rather than the specific earth station location. The frequency reuse feed and feed transport assembly installed in the CONSAT Laboratories MBTA are shown in Figure 3-18. The feed assembly support and foundation can be physically separate from the outer walls of the feed tower enclosure to reduce the effect of wind and thermal deformations on beam pointing.

In addition to the baseline 27-ft MBTA geometry, the 48-ft MBTA ($D/R = 0.3$) geometry, which provides 59-dB receive X-band gain, was also considered for RF analysis and costing. Figure 3-19 shows both the 27- and 48-ft MBTA geometries for the CONSAT Laboratories siting parameters in Table 3-1.

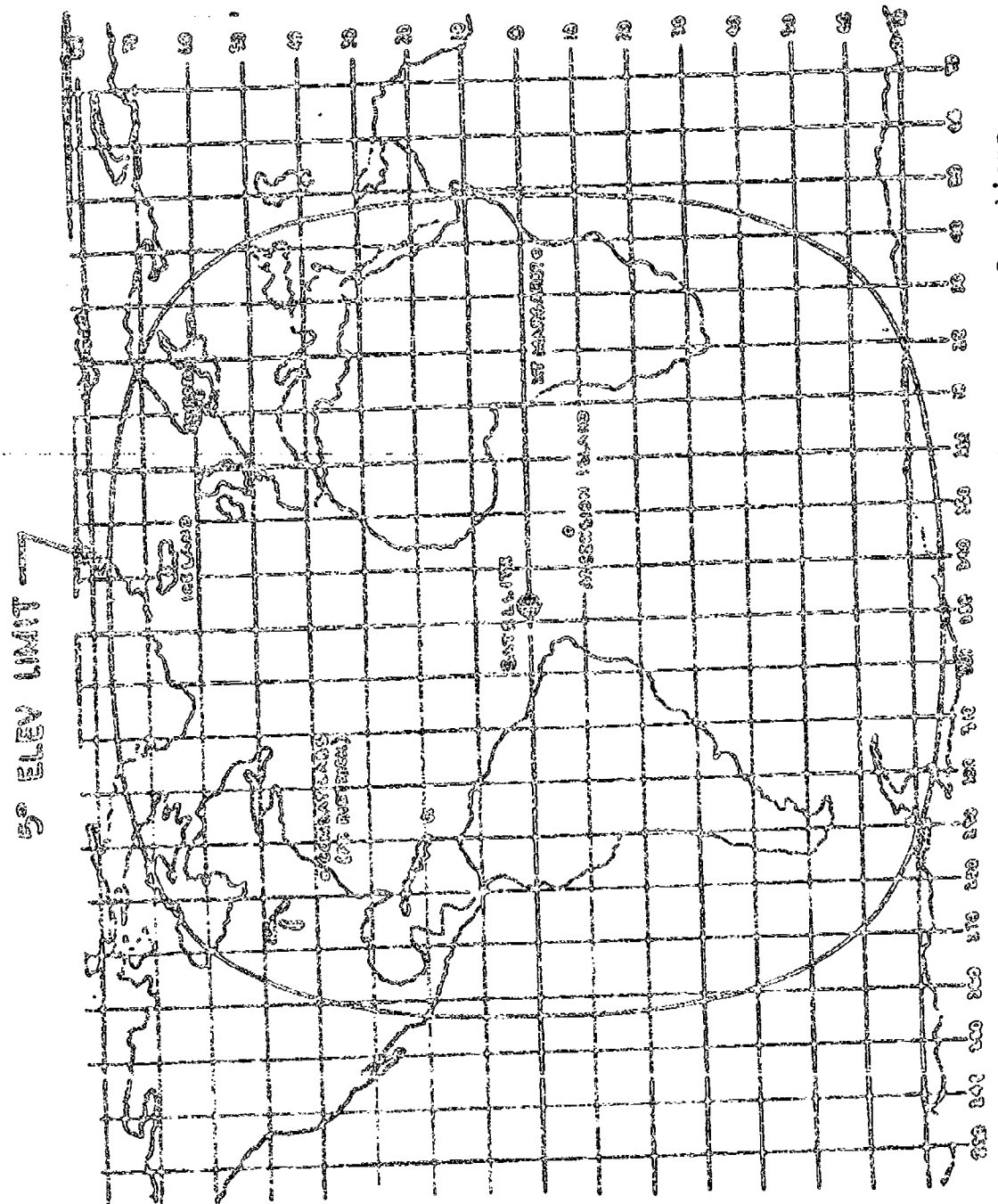


FIGURE 3-23. Widely deployed Reproductively Antenna 2G/3G.

Central Satellite Location 333 East Longitude all cases
Earth Station Location 2

Sweden
Latitude 60 North
Longitude 13 East

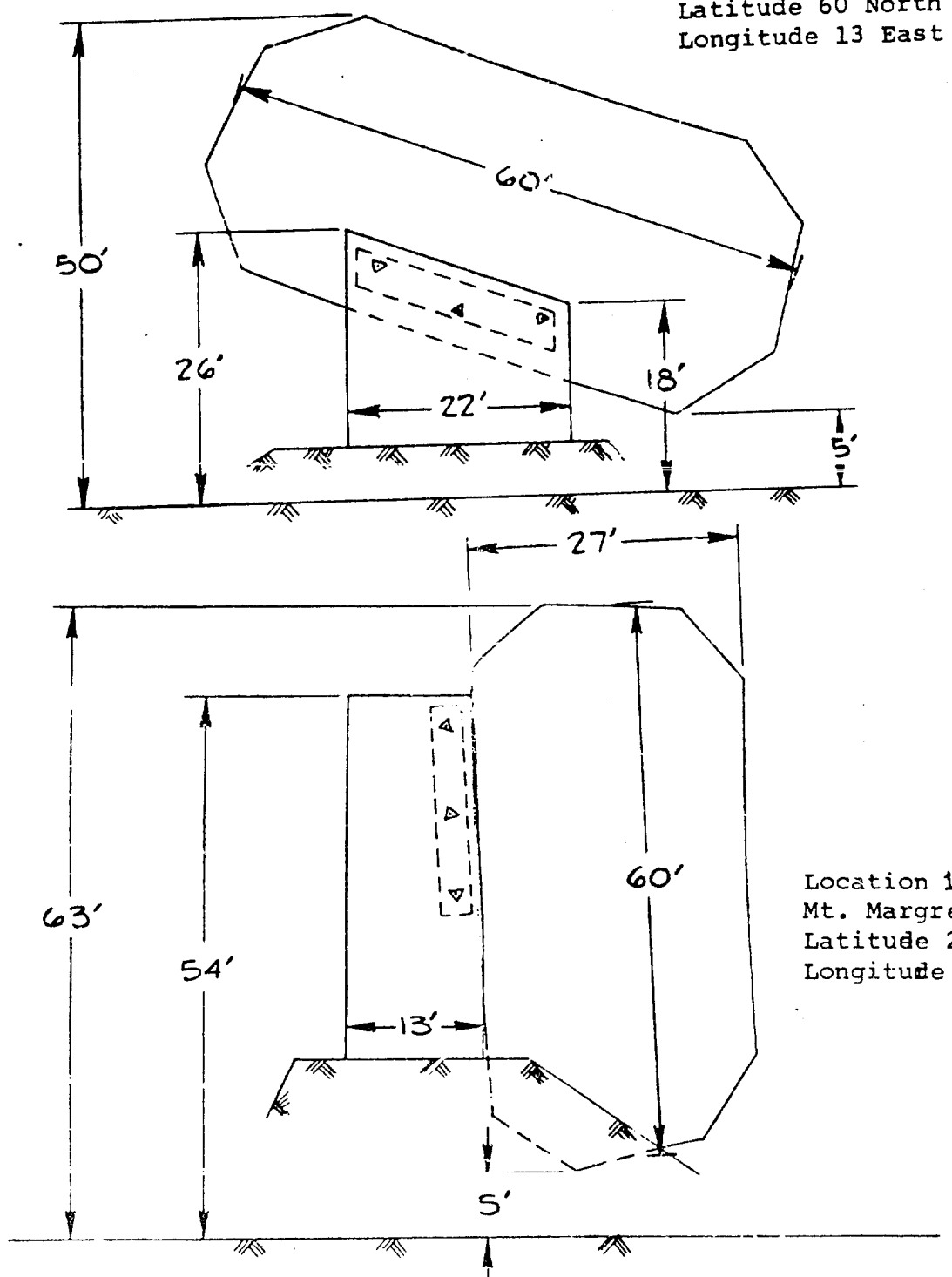
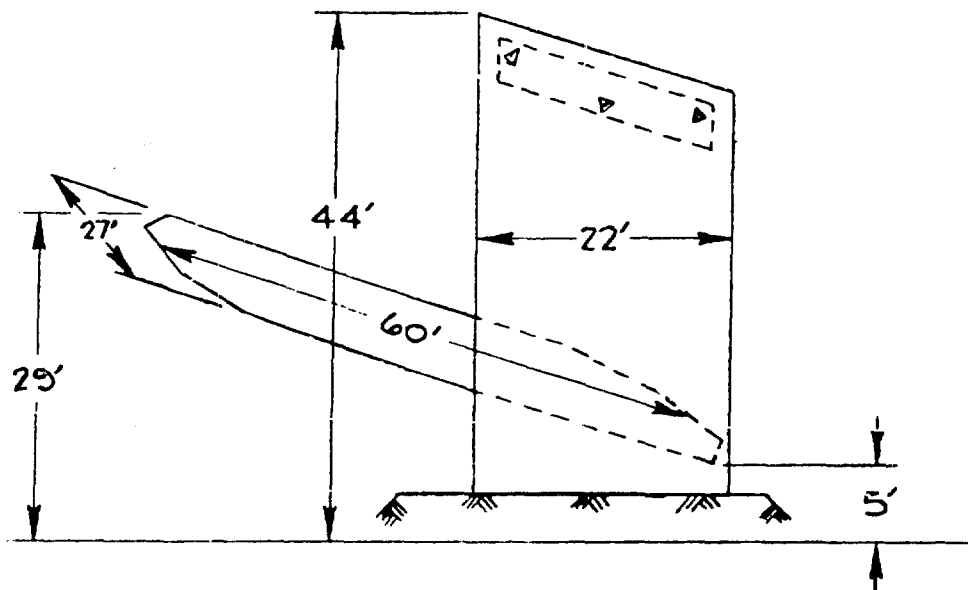


Figure 3-14. Views of MBTA at Sweden and Mt. Margaret
($\phi_{sat} = 333^\circ$ east longitude)

Earth Station Location 4: Ascension Island
Latitude 7 North
Longitude 346 East



Earth Station Location 3: Iceland
Latitude 66 North
Longitude 340 East

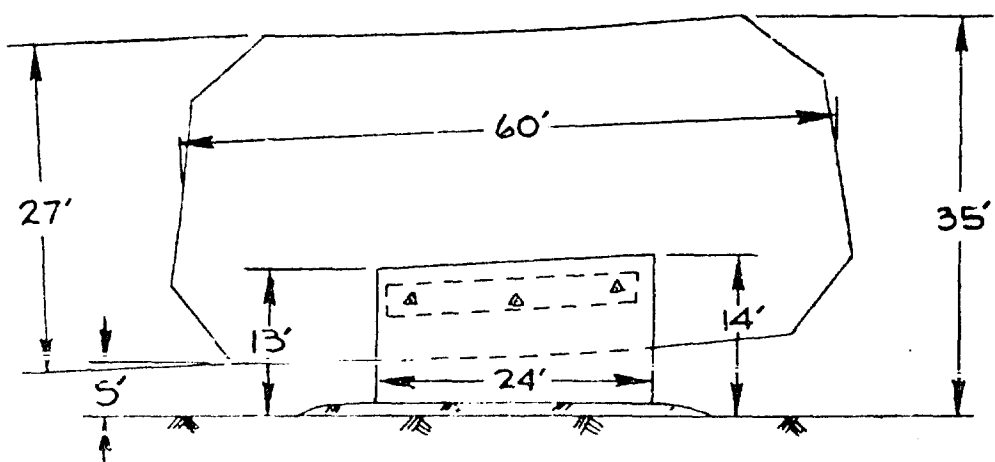


Figure 3-15. Views of MBTA at Ascension Island and Iceland
(ϕ_{sat} = 333° east longitude)

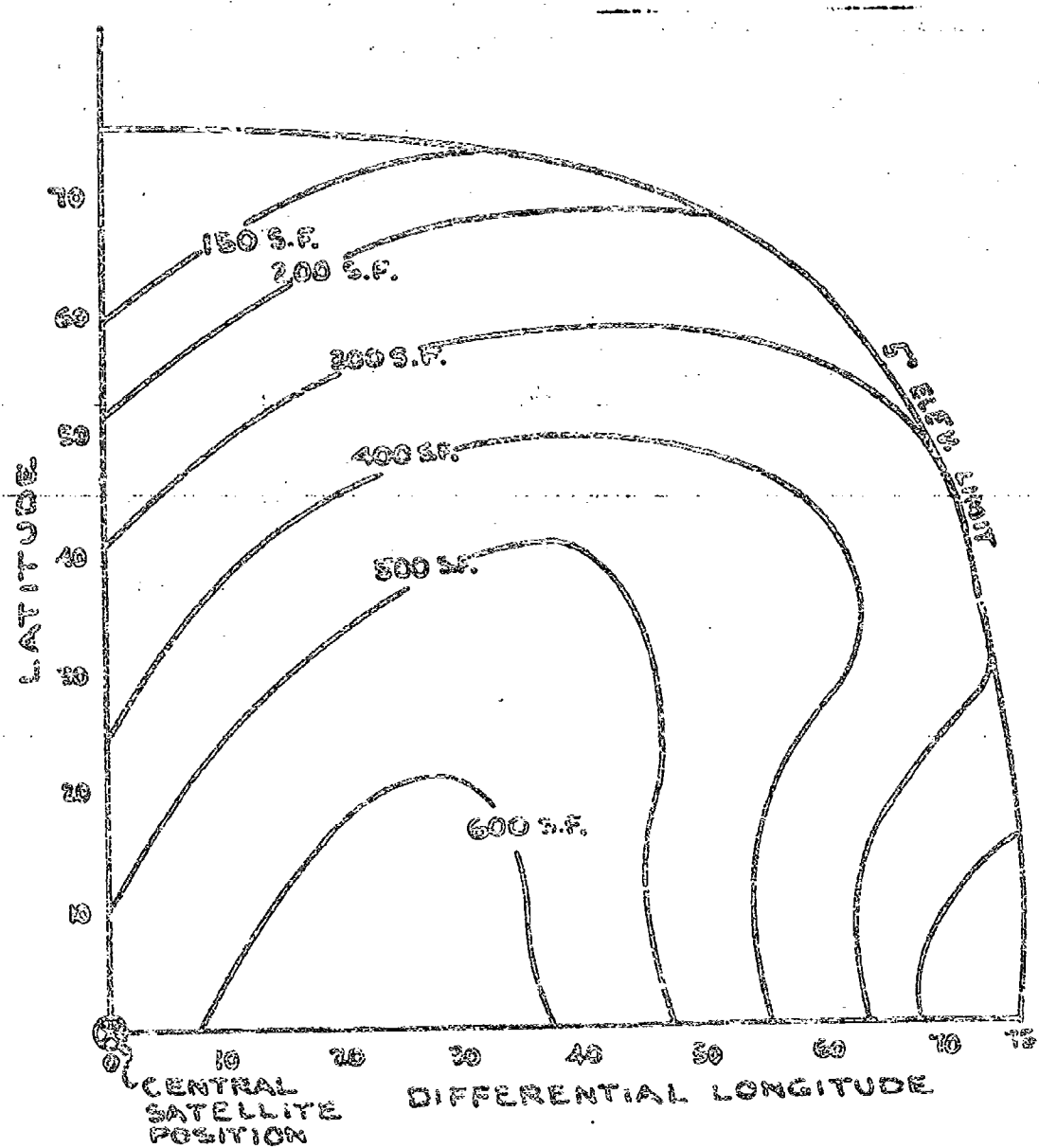
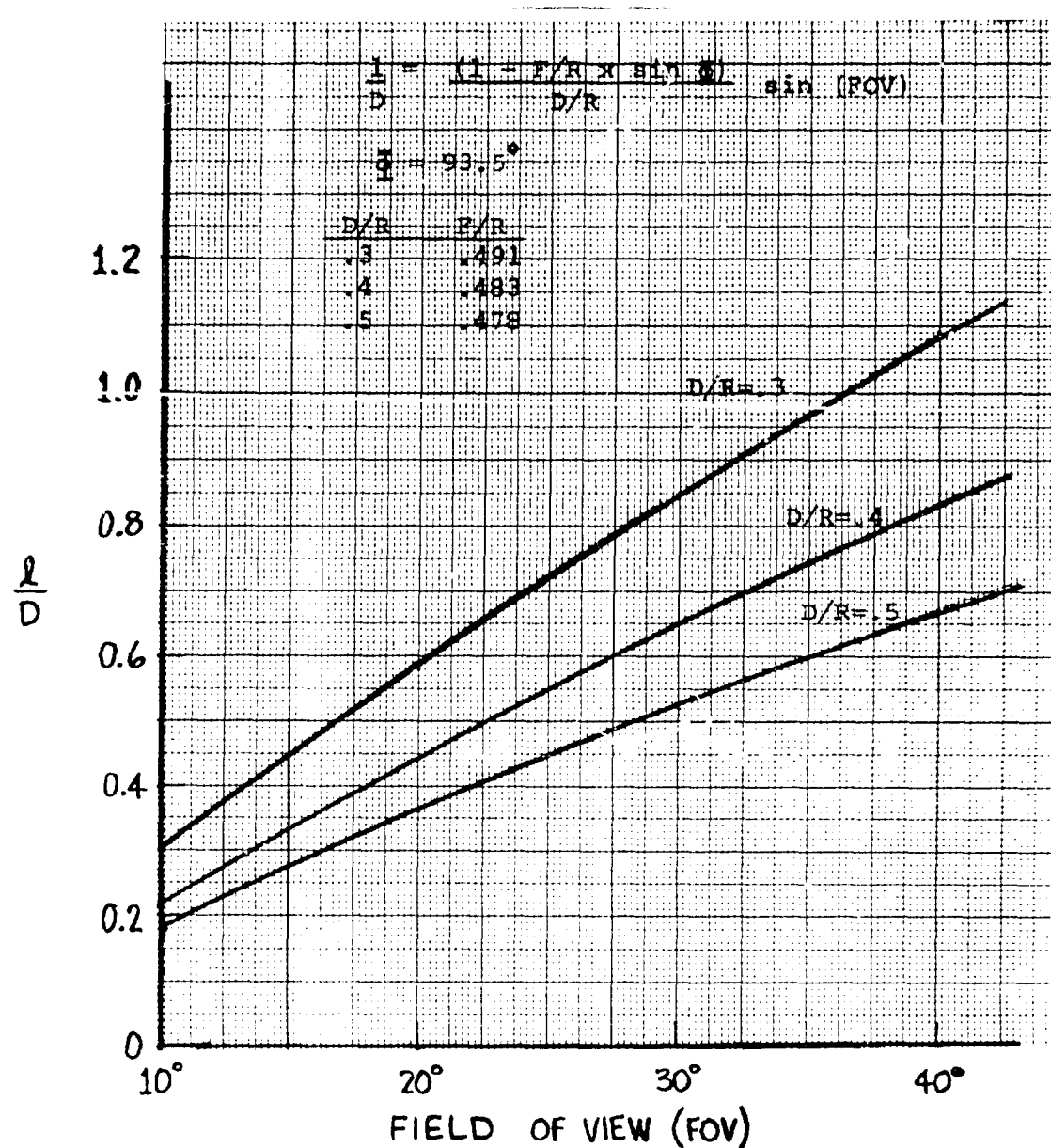


Figure 3-16. Feed Tower Width x Maximum Height
versus AZTA Location

Figure 3-17. Projected Feed ARC Length, ℓ/D

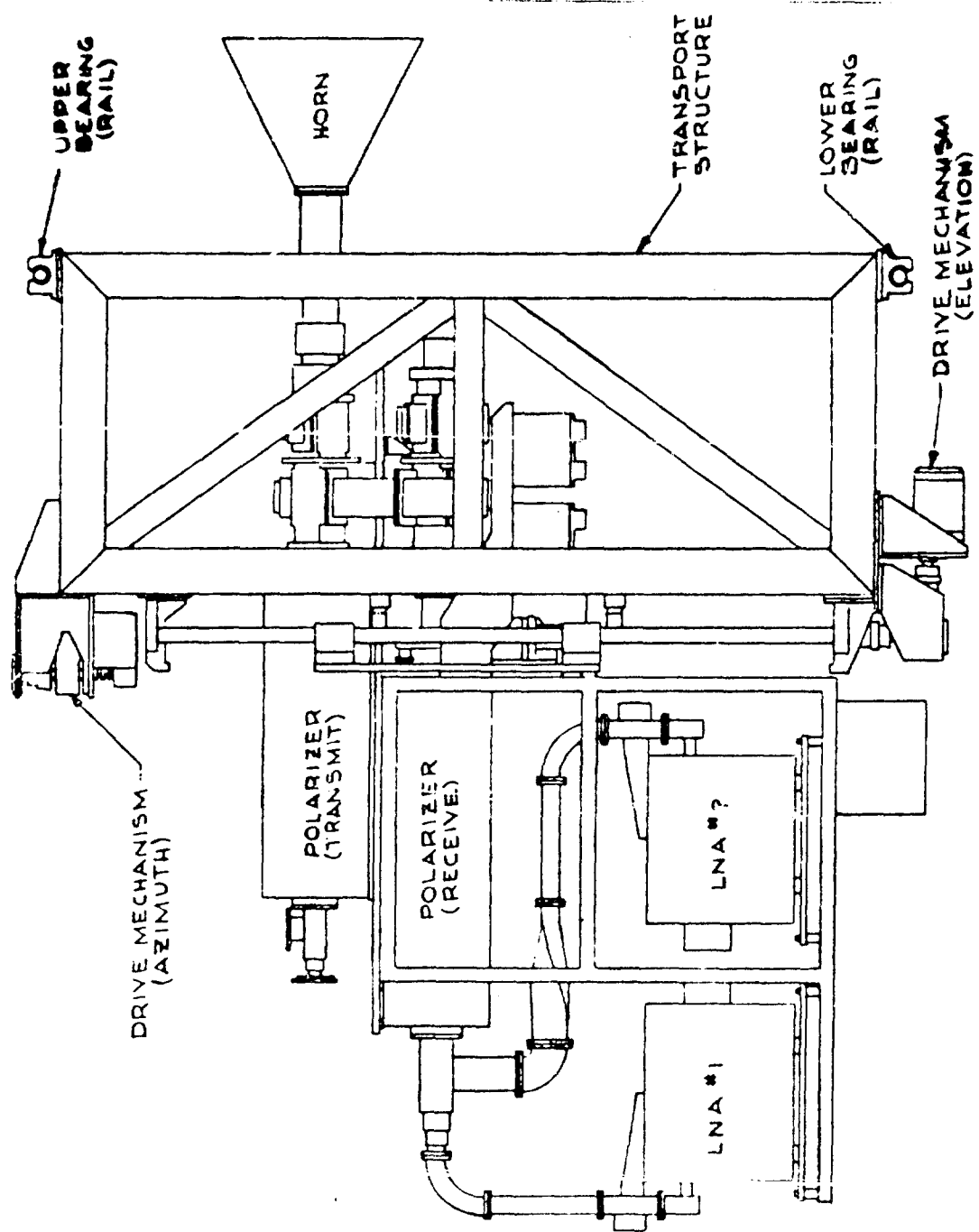


Figure 3-18. Feed Transport Assembly

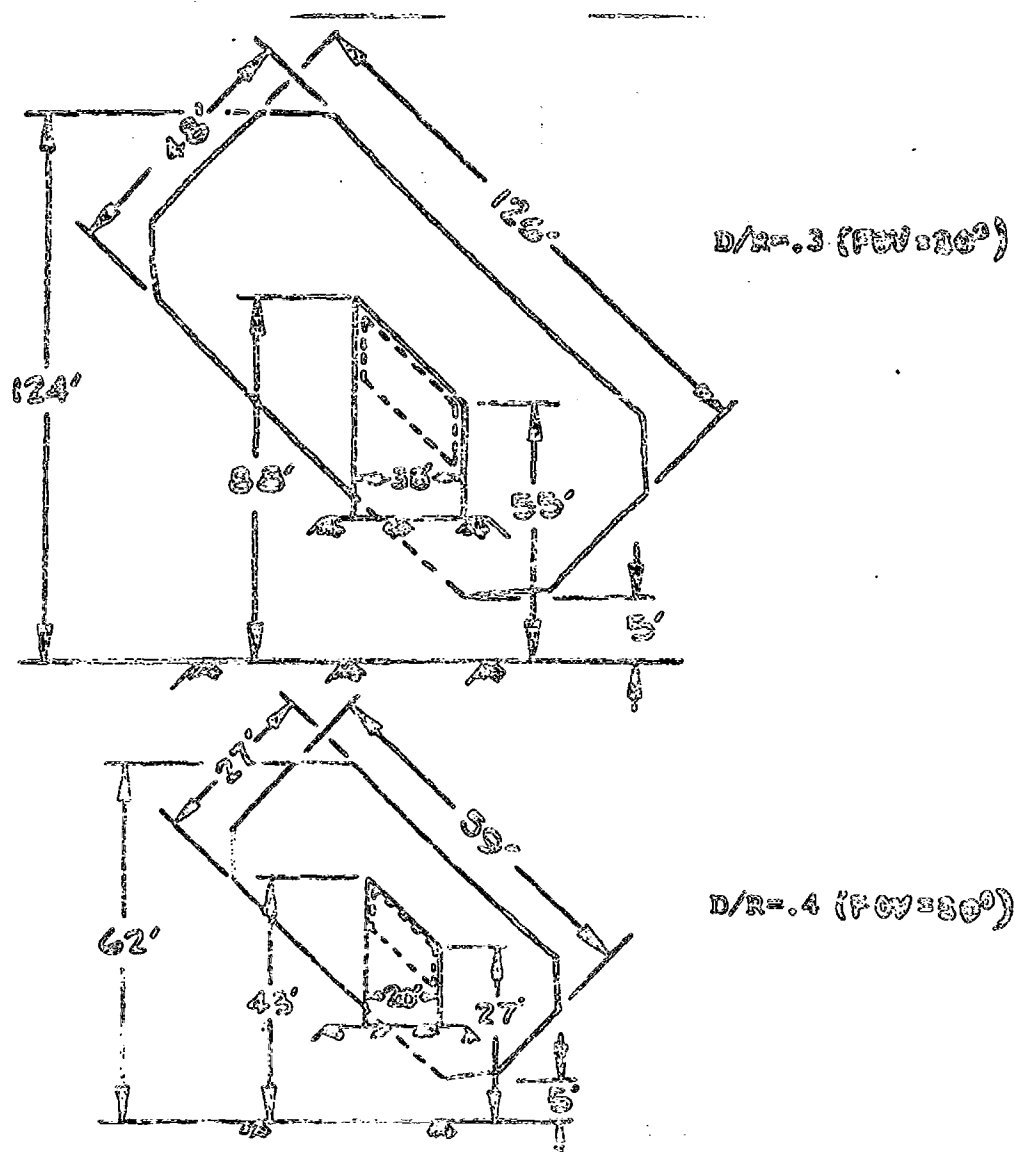


Figure 3-19. Views of 27-ft diameter ($D/R = 0.4$) and 48-ft diameter ($D/R = 0.3$) NEMA Geometries at CORFAT Laboratories

Figure 3-20 summarizes the total fabrication and implementation costs for the MBTA as a function of diameter for 0.020- and 0.040-inch operational surface tolerances. Electronic equipment (HPAs and LMRs) is not included. Cost estimates for fabrication and erection are derived from COMSAT's experience in implementing a 32- x 55-ft MBTA. Fabrication, erection, and foundation costs are a function of the aperture area (W x D) and the operational surface tolerance requirement. Foundation costs are based on a volume proportional to the area and height of the reflector scaled from the COMSAT Laboratories MBTA. The foundation, feed building, and transport rail costs are based on 1977 construction cost data. De-icing costs have not been included in Figure 3-20. COMSAT Laboratories' MBTA has operated successfully for 5 years without de-icing equipment. At high latitudes ($|\nu| > 40^\circ$) the reflector surface is nearly vertical and snow and ice accumulation is minimal.

The cost differentials between different MBTA locations are estimated to be less than 10 percent. The estimated cost for the baseline MBTA with a 30° field of view and 0.040-inch rms surface tolerance is

$$\text{baseline MBTA cost} = \$220,000 \quad (3-3)$$

Table 3-2 summarizes the baseline MBTA costs at four locations noted in Figure 3-13.

3.3 MBS 1: MBTA CHARACTERISTICS AT GOVERNMENT SATELLITE COMMUNICATIONS FREQUENCIES

The results of this study applied to task 1a are summarized in Table 3-3. The 27-ft-diameter baseline MBTA provides 34-dB receive band gain, and a 30° field of view with the

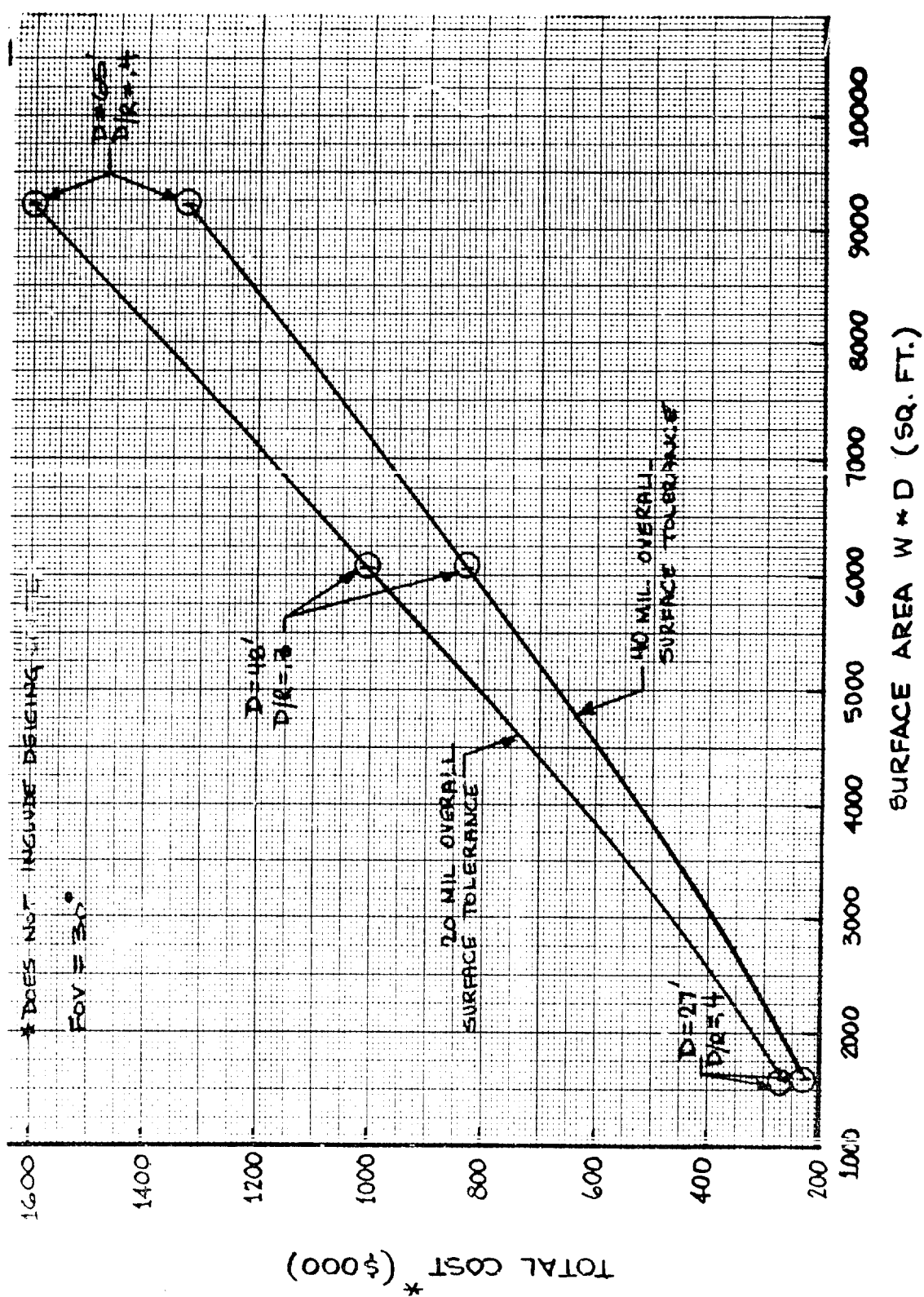


Figure 3-20. MBTA Costs versus Size and Operational Surface Tolerance

Table 3-2. 27-ft MBT Dimensions and Cost
at Several Locations

	St. Margaret	Sweden	Iceland	Ascooster I.
Latitude (deg)	-3	60	66	?
E. Longitude (deg)	37	13	360	346
Reflector Height (ft)	63	50	35	29
Reflector Foundation (yd ³)	22	23	16	13
Feed Building				
Width (ft)	12	12	12	22
Length (ft)	12	22	24	15
Height (ft)	34	26	16	44
Foundation (yd ³)	3	3	5	6
Feed Transport				
Width (ft)	6	17	18	27
Height (ft)	17	6	1	3
Cost (\$K)				
Fabrication	160	160	160	160
Erection	40.3	35.1	31.3	29.4
Foundation	5.4	5.1	3.6	2.9
Building	3.6	3.9	4.7	6.4
Transport	12	12	12	12
Total	224	219	212	213

TABLE 3-3. RISK 1.0: SURVIVAL OF INSULATING MATERIALS BY RADIATION

	2000 MeV RETA 1	2000 MeV RETA 2
External Dosimeter	17.6	27.6
Field of View	180	360
Minimum Aperture Dimensions 10/8 x 0.6	23 x 60 ft	27 x 60 ft
Operational and Success Tolerance	0.005 A.R.	0.013 A.R.
Operating Voltage (D/C = 100)	24.2 dB	34.2 dB
Efficiency Level	0.33 dB	0.13 dB
Operational and Survival Tolerance Level at 2.25 GeV	0.33 dB	0.13 dB
Survival Level over 10° Field of View	0.2 dB	0.1 dB
External Field Multi-Power Tolerance	0.35 x 0.16°	0.35 x 0.16°
Blank Electrical Level	<20 dB	<18 dB
External Gain Envelope	16 - 16 LOG: 1	12 - 16 LOG: 1
ROSS Gain/DCW Interaction Locates	0.1 dB	0.1 dB
ROSS Cross Polarization, 10° Offset	<13 dB	<13 dB
High-Current Beamwidth		
High-Current Beamwidth Tolerance	<0.1 dB	<0.1 dB
Reverberating Gain Margination		
ROSS/External Tolerance, G/T		
ROSS/External Temperature, T = 123°	11.9 dB/K	11.5 dB/K
10° Direction	<20 LOG 12/7.25 LOG	<22 LOG 16/7.35 LOG
0° Direction	<20 LOG 12/7.25 LOG	<20 LOG 16/7.35 LOG
ROSS/Growth (Repetitive) Power	<0.1 dB	<0.1 dB
Survival Tolerance 1.0, 25°, Gain Power		

$D/R = 0.4$ geometry results in a projected aperture diameter of 27×60 ft. The structural design was analyzed for operational RMS surface tolerances of 0.020 and 0.040 in. Operation of the NSRA at 11/14 and 28/30 GHz favors the use of the lower RMS surface tolerance. Figure 3-8 summarizes the multi-band (3.7- to 31-GHz) gain performance of the baseline NSRA.

Feed horns/OMTs are located close to the LNBs and NPBs in the NSRA concept. Feed systems can be electroformed as 1-piece units to eliminate metal-to-metal junctions which can give rise to nonlinear junction effects and resultant intermodulation products. Program or step-track systems may also be used to avoid complex nonpulse feed systems which could give rise to intermodulation effects. The individual panels in the reflector are electrically isolated to avoid intermodulation products.

North-south stationkeeping of $\pm 0.25^\circ$ yields less than 0.1 dB of parabolic plane scan loss. The maximum parabolic plane scan loss for $\pm 2.5^\circ$ of north-south scan is 2 dB.

The study results for task 1b have indicated that aberration-corrective subreflector/feed systems to compensate for spherical aberration are not required for the 54- to 59-dB receive band gain of interest to DS/CS. Studies at COMSAT Laboratories have shown that, to realize a reasonably symmetric subreflector design (as viewed from the feed), the parabolic and spherical foci of the NSRA must be displaced in a reflector which uses a correcting subreflector. A corrective subreflector concept must then be used for all frequency bands, since front feeding this reflector design results in unacceptably low efficiency.

The disadvantages associated with the correcting subreflector outweigh the advantages for medium gain (54- to 59-dB) NSRA systems. The first disadvantage is the mechanical complexity of the feed/subreflector system. The feed and subreflector must

be carefully aligned and must maintain their alignment while both travel on radii of curvature to scan the beam. The minimum beam spacing along the geosynchronous arc also increases. The diameter of the correcting subreflector determines the mechanical limit on beam spacing. However, a minimum beam spacing of 4° would still be feasible. North-south stationkeeping is also more difficult with the correcting subreflector design. Ideally both the feed and subreflector should scan as a fixed assembly in the parabolic plane. Scanning the feed alone would result in increased scan gain loss.

Task 1c required the determination of baseline NSPA performance in the 20/36-GHz band. Figure 3-8 shows that the baseline D/R = 0.4 design cost optimized for X-band coverage provides 59.5-dB gain at 20 GHz and 60.9-dB gain at 36 GHz with a 0.020-inch operational surface tolerance. A D/R = 0.3 geometry would yield 62-dB gain at 20 GHz and 63.5-dB gain at 36 GHz with a 0.020-inch operational surface tolerance. With a 30° field of view requirement, the aperture dimensions for the D/R = 0.3 geometry become 27 x 71.5 ft. North-south stationkeeping of ±0.25° corresponds to approximately three beamwidths of scan at 36 GHz, resulting in 0.5-dB parabolic plane scan loss.

3.4

TASK 2: NSPA CHARACTERISTICS FOR COMBINED OPERATION
AT BOTH GOVERNMENT AND COMMERCIAL SATELLITE FREQUENCIES

The study results applied to task 2 indicate that there is no performance impact on government X-band operation of the baseline NSPA when a second feed assembly is utilized to access a commercial 4/6- or 11/14-GHz satellite. The baseline antenna provides 48.2-dB gain at 3.7 GHz and 56-dB gain at 10.95 GHz with a 0.040-inch surface tolerance or 56.5-dB gain at 10.95 GHz with a 0.020-inch surface tolerance. The antenna temperature

characteristics are nearly identical for the 4/6-, 7/8-, and 11/14-GHz bands.

The cost impact of additional frequency bands is related to the cost of a new feed horn/OMT system and the associated electronics equipment. An identical feed transport assembly may be used for all frequency bands. The only variation in the entire MSTA system is the feed horn and associated electronics required to combine commercial operation (via a separate satellite) with government X-band operation. Since corrugated feed horns eliminate feed coupling effects, adjacent beam coupling can be determined solely from the secondary patterns of the MSTA at the different frequency bands.

3.5 TASK 3: MSTA MECHANICAL AND STRUCTURAL CHARACTERISTICS
REQUIRED FOR A WORLDWIDE DEPLOYMENT SYSTEM

The study results applied to task 3 show that a single reflector design ($\epsilon_r = 93.5^{\circ}$) is sufficient for a widely deployed DSCS system, thereby minimizing system fabrication costs. This single reflector design results in less than 0.3° of worst-case beam pointing error with spherical, one scan over a 40° field of view. This represents less than one to two beamwidths of required parabolic plane scan for exact beam repositioning in MSTA's having 54- to 59-dB gain and results in a negligible impact on RF performance. The identical reflector surface is utilized at all MSTA locations. The reflector support structure lengths vary to accommodate different MSTA latitudes and longitudes. The MSTA structure is engineered so that worldwide deployment results in no significant variations in electrical performance. (Beam scan loss varies slightly with different antenna latitudes as shown in Figure 3-12.)

The modular design of the MBTA reflector and structure permits the system to be easily transported and erected. All components are designed to a size that is readily transported by aircraft or truck.

The cost variation of the baseline MBTA as a function of antenna location is estimated to be less than 10 percent. A significant feature of the design is that it permits the MBTA to simultaneously serve several satellites over a fixed portion of the geostationary arc at different frequency bands. Only the feed system and electronics vary with frequency.

3.6

TASK 4: COST ESTIMATES FOR A RECOVERABLE MBTA

Cost estimates prepared for the baseline 27-ft-diameter MBTA ($D/R = 0.4$), which provides 54-dB down-link gain at 7.25 GHz with a 30° field of view, yield an antenna system cost of \$220,000 with a ±5-percent variation as a function of differential siting. The base cost is for a single beam. Addition of second (and subsequent) beams requires only a second feed system and feed transport assembly. A primary advantage of the MBTA concept is that additional beams at one or more frequency bands can be added at little additional cost. Because of the proximity of the feeds on the radial feed arc, redundant electronic units can be shared in multibeam operation. A third high-power amplifier or low-noise receiver can be utilized as the redundant backup unit for either beam in a 2-beam X-band system. The decreasing number of redundant electronic units required with an increasing number of active beams can result in significant overall system cost savings.

The baseline antenna provides more than 48-dB gain at 3.7 GHz. The cost of a dual beam system with one X-band and one C-band beam is identical to that noted above.

The baseline antenna with a 0.020-inch operating surface tolerance may be used for a dual beam system which provides a beam at X-band and a beam at K-band. The incremental cost is \$40,000 for a reflector structure with 0.020- rather than 0.040-inch operating rms surface tolerance. The baseline MBTA provides 59.5-dB gain at 20 GHz and 60.9-dB gain at 30 GHz. A D/R = 0.3 geometry of aperture dimensions 27 x 71.5 ft provides 62-dB gain at 20 GHz and 63.5-dB gain at 30 GHz, and the aperture area increase is 12 percent. A conservative incremental cost estimate for this MBTA geometry is \$44,000.

The 48-ft-diameter dual-beam MBTA (D/R = 0.3) provides 59-dB down-link gain at 7.25 GHz. The cost estimate for this MBTA is \$1,004,000 with a 0.020-inch operating surface tolerance and \$824,000 with a 0.040-inch operating surface tolerance. The cost increment for additional beams is only the cost of the feed system and its associated electronics.

3.7 CONCLUSIONS

The MBTA provides low sidelobes and a multibeam-multi-frequency capability in a simple, rugged, and reliable mechanical structure. Its modular design facilitates transportation and erection. The offset-fed MBTA provides low wide-angle sidelobe characteristics as a result of a blockage-free aperture. The formation of multiple beams at one or more frequency bands using shared apertures on a fixed reflector structure can result in significant cost savings in systems in which satellites are constrained to a fixed portion of the geosynchronous arc. Additional beams require only a relatively inexpensive feed system and

feed transport assembly. Redundant electronic equipment can be shared between multiple beams to further increase overall system economy.

For a given antenna gain, a single reflector structure is applicable to all DFCS antenna locations. The torus feed building incorporates all of the earth station elements except the reflector. Thus, feeds, receivers, transmitters, and other communications equipment and power supplies are all contained in a locked structure. No external devices are visible. The feed window may be optically opaque (but RF transparent) to conceal the antenna pointing and frequency band and hence the satellite(s) being utilized. The antenna system is much less sensitive to stray or intentional destruction (i.e., hunters' bullets) than conventional antenna systems with exposed waveguide runs or feed horns. Also, power and communications connections may be underground.

The multiple-beam feed assembly permits immediate transfer of communications traffic if a fault occurs. Critical traffic can easily be handled in two redundant paths to two satellites without increasing reflector system cost. Thus, no-break communication is possible with one reflector.

Relative to conventional fully steerable Cassegrain reflectors, the MSTA offers the following performance advantages:

- a. lower sidelobes;
- b. lower antenna noise temperature;
- c. a more rigid fixed reflector and a lightweight feed assembly, allowing lower inertia tracking and hence greater tracking accuracy;
- d. less maintenance as a result of eliminating large gears, bearings, and motors;

- e. low power consumption since fractional horse-power motors move the feed/LNA assembly;
- f. the use of one for a redundant electronics equipment among two or more separate beams to permit increased reliability or reduced costs for a given level of reliability;
- g. simplification of frequency band changes; and
- h. simple optics since subreflector adjustments are not required.

The one major disadvantage of the fixed reflector MFTA is the lack of pointing flexibility. The antenna system is designed to track satellites only over a fixed portion of the geosynchronous arc. However, in communications satellite systems with well defined orbital positions and ranges of satellites, the cost savings and performance advantages of the MFTA system can be considerable.